MIMO Broadcasting for Simultaneous Wireless Information and Power Transfer

Rui Zhang and Chin Keong Ho

Abstract

Wireless power transfer (WPT) is a promising new solution to provide convenient and perpetual energy supplies to wireless networks. In practice, WPT is implementable by various technologies such as inductive coupling, magnetic resonate coupling, and electromagnetic (EM) radiation, for short-/mid-/long-range applications, respectively. In this paper, we consider the EM or radio signal enabled WPT in particular. Since radio signals can carry energy as well as information at the same time, a unified study on *simultaneous wireless information and power transfer* (SWIPT) is pursued. Specifically, this paper studies a multiple-input multiple-output (MIMO) wireless broadcast system consisting of three nodes, where one receiver harvests energy and another receiver decodes information separately from the signals sent by a common transmitter, and all the transmitter and receivers may be equipped with multiple antennas. Two scenarios are examined, in which the information receiver and energy receiver are *separated* and see different MIMO channels from the transmitter, or *co-located* and see the identical MIMO channel from the transmitter. For the case of separated receivers, we derive the optimal transmission strategy to achieve different tradeoffs for maximal information rate versus energy transfer, which are characterized by the boundary of a so-called *rate-energy* (R-E) region. For the case of co-located receivers, we show an outer bound for the achievable R-E region due to the potential limitation that practical energy harvesting receivers are not yet able to decode information directly. Under this constraint, we investigate two practical designs for the co-located receiver case, namely *time switching* and *power splitting*, and characterize their achievable R-E regions in comparison to the outer bound.

Index Terms

MIMO system, broadcast channel, precoding, wireless power, simultaneous wireless information and power transfer (SWIPT), rate-energy tradeoff, energy harvesting.

I. INTRODUCTION

Energy-constrained wireless networks, such as sensor networks, are typically powered by batteries that have limited operation time. Although replacing or recharging the batteries can prolong the lifetime of the network to a certain extent, it usually incurs high costs and is inconvenient, hazardous (say, in toxic environments), or even impossible (e.g., for sensors embedded in building structures or inside human bodies). A more convenient, safer, as well as "greener" alternative is thus to harvest energy from the environment, which virtually provides perpetual

energy supplies to wireless devices. In addition to other commonly used energy sources such as solar and wind, ambient radio-frequency (RF) signals can be a viable new source for energy scavenging. It is worth noting that RF-based energy harvesting is typically suitable for low-power applications (e.g., sensor networks), but also can be applied for scenarios with more substantial power consumptions if dedicated wireless power transmission is implemented.[1]

On the other hand, since RF signals that carry energy can at the same time be used as a vehicle for transporting information, *simultaneous wireless information and power transfer* (SWIPT) becomes an interesting new area of research that attracts increasing attention. Although a unified study on this topic is still in the infancy stage, there have been notable results reported in the literature [1], [2]. In [1], Varshney first proposed a *capacity-energy* function to characterize the fundamental tradeoffs in simultaneous information and energy transfer. For the single-antenna or SISO (single-input single-output) AWGN (additive white Gaussian noise) channel with amplitude-constrained inputs, it was shown in [1] that there exist nontrivial tradeoffs in maximizing information rate versus (vs.) power transfer by optimizing the input distribution. However, if the average transmit-power constraint is considered instead, the above two goals can be shown to be aligned for the SISO AWGN channel with Gaussian input signals, and thus there is no nontrivial tradeoff. In [2], Grover and Sahai extended [1] to frequency-selective single-antenna AWGN channels with the average power constraint, by showing that a non-trivial tradeoff exists in frequency-domain power allocation for maximal information vs. energy transfer.

As a matter of fact, *wireless power transfer* (WPT) or in short *wireless power*, which generally refers to the transmissions of electrical energy from a power source to one or more electrical loads without any interconnecting wires, has been investigated and implemented with a long history. Generally speaking, WPT is carried out using either the "near-field" electromagnetic (EM) induction (e.g., inductive coupling, capacitive coupling) for short-distance (say, less than a meter) applications such as passive radio-frequency identification (RFID) [3], or the "far-field" EM radiation in the form of microwaves or lasers for long-range (up to a few kilometers) applications such as the transmissions of energy from orbiting solar power satellites to Earth or spacecrafts [4]. However, prior research on EM radiation based WPT, in particular over the RF band, has been pursued independently from that on wireless information transfer (WIT) or radio communication. This is non-surprising since these two lines of work in general have very different research goals: WIT is to maximize the *information transmission capacity* of wireless channels subject to channel impairments such as the fading and receiver noise, while WPT is to maximize the *energy transmission efficiency* (defined as the ratio of the energy harvested and stored at the receiver to that consumed by the transmitter) over a wireless medium. Nevertheless, it is worth noting that the design objectives

---

[1]Interested readers may visit the company website of Powercast at http://www.powercastco.com/ for more information on recent applications of dedicated RF-based power transfer.
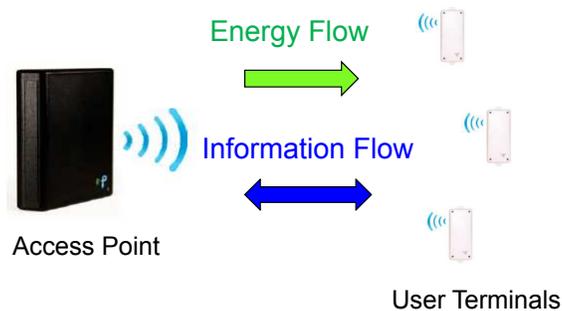
Fig. 1.   A wireless network with dual information and energy transfer.

for WPT and WIT systems can be aligned, since given a transmitter energy budget, maximizing the signal power received (for WPT) is also beneficial in maximizing the channel capacity (for WIT) against the receiver noise.

Hence, in this paper we attempt to pursue a unified study on WIT and WPT for emerging wireless applications with such a dual usage. An example of such wireless dual networks is envisaged in Fig. 1, where a fixed access point (AP) coordinates the two-way communications to/from a set of distributed user terminals (UTs). However, unlike the conventional wireless network in which both the AP and UTs draw energy from constant power supplies (by e.g. connecting to the grid or a battery), in our model, only the AP is assumed to have a constant power source, while all UTs need to replenish energy from the received signals sent by the AP via the far-field RF-based WPT. Consequently, the AP needs to coordinate the wireless information and energy transfer to UTs in the downlink, in addition to the information transfer from UTs in the uplink. Wireless networks with such a dual information and power transfer feature have not yet been studied in the literature to our best knowledge, although some of their interesting applications have already appeared in, e.g., the body sensor networks [5] with the out-body local processing units (LPUs) powered by battery communicating and at the same time sending wireless power to in-body sensors that have no embedded power supplies. However, how to characterize the fundamental information-energy transmission tradeoff in such dual networks is still an open problem.

In this paper, we focus our study on the downlink case with simultaneous WIT and WPT from the AP to UTs. In the generic system model depicted in Fig. 1, each UT can in general harvest energy and decode information at the same time (by e.g. applying the power splitting scheme introduced later in this paper). However, from an implementation viewpoint, one particular design whereby each UT operates as either an information receiver or an energy receiver at any given time may be desirable, which is referred to as *time switching*. This scheme is practically appealing since state-of-the-art wireless information and energy receivers are typically designed to operate separately with very different power sensitivities (e.g., -50dBm for information receivers vs. -10dBm for energy receivers). As a result, if time switching is employed at each UT jointly with the "near-far" based

transmission scheduling at the AP, i.e., UTs that are close to the AP and thus receive high power from the AP are scheduled for WET, whereas those that are more distant from the AP and thus receive lower power are scheduled for WIT, then SWIPT systems can be efficiently implemented with existing information and energy receivers and the additional time-switching device at each receiver.

For an initial study on SWIPT, this paper considers the simplified scenarios with only one or two active UTs in the network at any given time. For the case of two UTs, we assume time switching, i.e., the two UTs take turns to receive energy or (independent) information from the AP over different time blocks. As a result, when one UT receives information from the AP, the other UT can opportunistically harvest energy from the same signal broadcast by the AP, and vice versa. Hence, at each block, one UT operates as an information decoding (ID) receiver, and the other UT as an energy harvesting (EH) receiver. We thus refer to this case as *separated EH and ID receivers*. On the other hand, for the case with only one single UT to be active at one time (while all other UTs are assumed to be in the off/sleep mode), the active UT needs to harvest energy as well as decode information from the same signal sent by the AP, i.e., the same set of receiving antennas are shared by both EH and ID receivers residing in the same UT. Thus, this case is referred to as *co-located EH and ID receivers*. Surprisingly, as we will show later in this paper, the optimal information-energy tradeoff for the case of co-located receivers is more challenging to characterize than that for the case of separated receivers, due to a potential limitation that practical EH receiver circuits are not yet able to decode the information directly and vice versa. Note that similar to the case of separated receives, time switching can also be applied in the case of co-located receivers to orthogonalize the information and energy transmissions at each receiving antenna; however, this scheme is in general suboptimal for the achievable rate-energy tradeoffs in the case of co-located receivers, as will be shown later in this paper.

Some further assumptions are made in this paper for the purpose of exposition. Firstly, this paper considers a quasi-static fading environment where the wireless channel between the AP and each UT is assumed to be constant over a sufficiently long period of time during which the number of transmitted symbols can be approximately regarded as being infinitely large. Under this assumption, we further assume that it is feasible for each UT to estimate the downlink channel from the AP and then send it back to the AP via the uplink, since the time overhead for such channel estimation and feedback is a negligible portion of the total transmission time due to quasi-static fading. We will address the more general case of fading channels with imperfect/partial channel knowledge at the transmitter in our future work. Secondly, we assume that the system under our study typically operates at the high signal-to-noise ratio (SNR) regime for the ID receiver in the case of co-located receivers. This is to be compatible with the high-power operating requirement for the EH receiver of practical interest as previously mentioned. Thirdly, without loss of generality, we assume a multi-antenna or MIMO (multiple-input multiple-output) system, in which
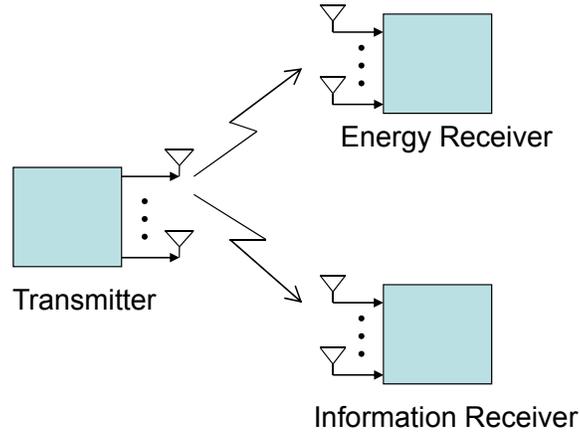
Fig. 2. A MIMO broadcast system for simultaneous wireless information and power transfer.

the AP is equipped with multiple antennas, and each UT is equipped with one or more antennas, for enabling both the high-performance wireless energy and information transmissions (as it is well known that for WIT only, MIMO systems can achieve folded array/capacity gains over SISO systems by spatial beamforming/multiplexing [6]).

Under the above assumptions, a three-node MIMO broadcast system is considered in this paper, as shown in Fig. 2, wherein the EH and ID receivers harvest energy and decode information separately from the signal sent by a common transmitter. Note that this system model refers to the case of separated EH and ID receivers in general, but includes the co-located receivers as a special case when the MIMO channels from the transmitter to both receivers become identical. Assuming this model, the main results of this paper are summarized as follows:

- For the case of separated EH and ID receivers, we design the optimal transmission strategy to achieve different tradeoffs between maximal information rate vs. energy transfer, which are characterized by the boundary of a so-called *rate-energy* (R-E) region. We derive a semi-closed-form expression for the optimal transmit covariance matrix (for the joint precoding and power allocation) to achieve different rate-energy pairs on the boundary of the R-E region. Note that the R-E region is a multiuser extension of the single-user capacity-energy function in [1]. Also note that the multi-antenna broadcast channel (BC) has been investigated in e.g. [7]–[12] for information transfer solely by unicasting or multicasting. However, MIMO-BC for SWIPT as considered in this paper is new and has not yet been studied by any prior work.

- For the case of co-located EH and ID receivers, we show that the proposed solution for the case of separated receivers is also applicable with the identical MIMO channel from the transmitter to both ID and EH receivers. Furthermore, we consider a potential practical constraint that EH receiver circuits cannot directly decode the information (i.e., any information embedded in received signals sent to the EH receiver is lost during the EH
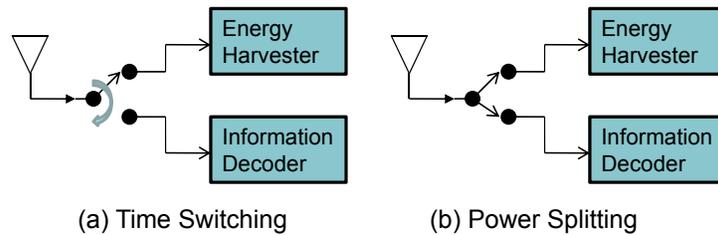
Fig. 3. Two practical designs for the co-located energy and information receivers, which are applied for each receiving antenna.

process). Under this constraint, we show that the R-E region with the optimal transmit covariance (obtained without such a constraint) in general only serves as a performance outer bound for the co-located receiver case.

- Hence, we investigate two practical receiver designs, namely *time switching* and *power splitting*, for the case of co-located receivers. As shown in Fig. 3, for time switching, each receiving antenna periodically switches between the EH receiver and ID receiver, whereas for power splitting, the received signal at each antenna is split into two separate signal streams with different power levels, one sent to the EH receiver and the other to the ID receiver. Note that time switching has also been proposed in [14] for the SISO AWGN channel. Furthermore, note that the *antenna switching* scheme whereby the receiving antennas are divided into two groups with one group switched to information decoding and the other group to energy harvesting can be regarded as a special case of power splitting with only binary splitting power ratios at each receiving antenna. For these practical receiver designs, we derive their achievable R-E regions as compared to the R-E region outer bound, and characterize the conditions under which their performance gaps can be closed. For example, we show that the power splitting scheme approaches the tradeoff upper bound asymptotically when the RF-band antenna noise at the receiver becomes more dominant over the baseband processing noise (more details are given in Section IV-C).

The rest of this paper is organized as follows: Section II presents the system model, characterizes the rate-energy region, and formulates the problem for finding the optimal transmit covariance matrix. Section III presents the optimal transmit covariance solution for the case of separated receivers. Section IV extends the solution to the case of co-located receivers to obtain a performance upper bound, proposes practical receiver designs, and analyzes their performance limits as compared to the performance upper bound. Finally, Section V concludes the paper and provides some promising directions for future work.

Notation: For a square matrix S, $\text{tr}(S)$, $|S|$, S^{-1}, and $S^{\frac{1}{2}}$ denote its trace, determinant, inverse, and square-root, respectively, while $S \succeq 0$ and $S \succ 0$ mean that S is positive semi-definite and positive definite, respectively.

For an arbitrary-size matrix $\boldsymbol{M}$, $\boldsymbol{M}^H$ and $\boldsymbol{M}^T$ denote the conjugate transpose and transpose of $\boldsymbol{M}$, respectively. $\mathrm{diag}(x_1, \ldots, x_M)$ denotes an $M \times M$ diagonal matrix with $x_1, \ldots, x_M$ being the diagonal elements. $\boldsymbol{I}$ and $\boldsymbol{0}$ denote an identity matrix and an all-zero vector, respectively, with appropriate dimensions. $\mathbb{E}[\cdot]$ denotes the statistical expectation. The distribution of a circularly symmetric complex Gaussian (CSCG) random vector with mean $\boldsymbol{x}$ and covariance matrix $\boldsymbol{\Sigma}$ is denoted by $\mathcal{CN}(\boldsymbol{x}, \boldsymbol{\Sigma})$, and $\sim$ stands for "distributed as". $\mathbb{C}^{x \times y}$ denotes the space of $x \times y$ matrices with complex entries. $\|\boldsymbol{z}\|$ is the Euclidean norm of a complex vector $\boldsymbol{z}$, and $|z|$ is the absolute value of a complex scalar z. $\max(x, y)$ and $\min(x, y)$ denote the maximum and minimum between two real numbers, x and y, respectively, and $(x)^+ = \max(x, 0)$. All the $\log(\cdot)$ functions have base-2 by default.

II. SYSTEM MODEL AND PROBLEM FORMULATION

As shown in Fig. 2, this paper considers a wireless broadcast system consisting of one transmitter, one EH receiver, and one ID receiver. It is assumed that the transmitter is equipped with $M \geq 1$ transmitting antennas, and the EH receiver and the ID receiver are equipped with $N_{\mathrm{EH}} \geq 1$ and $N_{\mathrm{ID}} \geq 1$ receiving antennas, respectively. In addition, it is assumed that the transmitter and both receivers operate over the same frequency band. Assuming a narrow-band transmission over quasi-static fading channels, the baseband equivalent channels from the transmitter to the EH receiver and ID receiver can be modeled by matrices $\boldsymbol{G} \in \mathbb{C}^{N_{\mathrm{EH}} \times M}$ and $\boldsymbol{H} \in \mathbb{C}^{N_{\mathrm{ID}} \times M}$, respectively. It is assumed that at each fading state, $\boldsymbol{G}$ and $\boldsymbol{H}$ are both known at the transmitter, and separately known at the corresponding receiver. Note that for the case of co-located EH and ID receivers, $\boldsymbol{G}$ is identical to $\boldsymbol{H}$ and thus $N_{\mathrm{EH}} = N_{\mathrm{ID}}$.

It is worth noting that the EH receiver does not need to convert the received signal from the RF band to the baseband in order to harvest the carried energy. Nevertheless, thanks to the law of energy conservation, it can be assumed that the total harvested RF-band power (energy normalized by the baseband symbol period), denoted by Q, from all receiving antennas at the EH receiver is proportional to that of the received baseband signal, i.e.,

$$Q = \zeta \mathbb{E}[\|\boldsymbol{G}\boldsymbol{x}(n)\|^2] \tag{1}$$

where ζ is a constant that accounts for the loss in the energy transducer for converting the harvested energy to electrical energy to be stored; for the convenience of analysis, it is assumed that $\zeta = 1$ in this paper unless stated otherwise. We use $\boldsymbol{x}(n) \in \mathbb{C}^{M \times 1}$ to denote the baseband signal broadcast by the transmitter at the nth symbol interval, which is assumed to be random over n, without loss of generality. The expectation in (1) is thus used to compute the average power harvested by the EH receiver at each fading state. Note that for simplicity, we assumed in (1) that the harvested energy due to the background noise at the EH receiver is negligible and thus can be

ignored.[2]

On the other hand, the baseband transmission from the transmitter to the ID receiver can be modeled by

$$\boldsymbol{y}(n) = \boldsymbol{H}\boldsymbol{x}(n) + \boldsymbol{z}(n) \tag{2}$$

where $\boldsymbol{y}(n) \in \mathbb{C}^{N_{\text{ID}} \times 1}$ denotes the received signal at the nth symbol interval, and $\boldsymbol{z}(n) \in \mathbb{C}^{N_{\text{ID}} \times 1}$ denotes the receiver noise vector. It is assumed that $\boldsymbol{z}(n)$'s are independent over n and $\boldsymbol{z}(n) \sim \mathcal{CN}(\boldsymbol{0}, \boldsymbol{I})$. Under the assumption that $\boldsymbol{x}(n)$ is random over n, we use $\boldsymbol{S} = \mathbb{E}[\boldsymbol{x}(n)\boldsymbol{x}^H(n)]$ to denote the covariance matrix of $\boldsymbol{x}(n)$. In addition, we assume that there is an average power constraint at the transmitter across all transmitting antennas denoted by $\mathbb{E}[\|\boldsymbol{x}(n)\|^2] = \text{tr}(\boldsymbol{S}) \leq P$. In the following, we examine the optimal transmit covariance $\boldsymbol{S}$ to maximize the transported energy efficiency and information rate to the EH and ID receivers, respectively.

Consider first the MIMO link from the transmitter to the EH receiver when the ID receiver is not present. In this case, the design objective for $\boldsymbol{S}$ is to maximize the power Q received at the EH receiver. Since from (1) it follows that $Q = \text{tr}(\boldsymbol{G}\boldsymbol{S}\boldsymbol{G}^H)$ with $\zeta = 1$, the aforementioned design problem can be formulated as

$$\text{(P1)} \quad \max_{\boldsymbol{S}} \quad Q := \text{tr}\left(\boldsymbol{G}\boldsymbol{S}\boldsymbol{G}^H\right)$$
$$\text{s.t.} \quad \text{tr}(\boldsymbol{S}) \leq P, \boldsymbol{S} \succeq 0.$$

Let $T_1 = \min(M, N_{\text{EH}})$ and the (reduced) singular value decomposition (SVD) of $\boldsymbol{G}$ be denoted by $\boldsymbol{G} = \boldsymbol{U}_G \boldsymbol{\Gamma}_G^{1/2} \boldsymbol{V}_G^H$, where $\boldsymbol{U}_G \in \mathbb{C}^{N_{\text{EH}} \times T_1}$ and $\boldsymbol{V}_G \in \mathbb{C}^{M \times T_1}$, each of which consists of orthogonal columns with unit norm, and $\boldsymbol{\Gamma}_G = \text{diag}(g_1, \ldots, g_{T_1})$ with $g_1 \geq g_2 \geq \ldots \geq g_{T_1} \geq 0$. Furthermore, let $\boldsymbol{v}_1$ denote the first column of $\boldsymbol{V}_G$. Then, we have the following proposition.

Proposition 2.1: The optimal solution to (P1) is $\boldsymbol{S}_{\text{EH}} = P\boldsymbol{v}_1\boldsymbol{v}_1^H$.

Proof: See Appendix A. ∎

Given $\boldsymbol{S} = \boldsymbol{S}_{\text{EH}}$, it follows that the maximum harvested power at the EH receiver is given by $Q_{\max} = g_1 P$. It is worth noting that since $\boldsymbol{S}_{\text{EH}}$ is a rank-one matrix, the maximum harvested power is achieved by *beamforming* at the transmitter, which aligns with the strongest eigenmode of the matrix $\boldsymbol{G}^H\boldsymbol{G}$, i.e., the transmitted signal can be written as $\boldsymbol{x}(n) = \sqrt{P}\boldsymbol{v}_1 s(n)$, where $s(n)$ is an arbitrary random signal over n with zero mean and unit variance, and $\boldsymbol{v}_1$ is the transmit beamforming vector. For convenience, we name the above transmit beamforming scheme to maximize the efficiency of WPT as "energy beamforming".

Next, consider the MIMO link from the transmitter to the ID receiver without the presence of any EH receiver. Assuming the optimal Gaussian codebook at the transmitter, i.e., $\boldsymbol{x}(n) \sim \mathcal{CN}(\boldsymbol{0}, \boldsymbol{S})$, the transmit covariance $\boldsymbol{S}$ to

---

[2]The results of this paper are readily extendible to study the impacts of non-negligible background noise and/or co-channel interference on the SWIPT system performance.

maximize the transmission rate over this MIMO channel can be obtained by solving the following problem [13]:

$$(\text{P2}) \quad \max_{\boldsymbol{S}} \quad R := \log |\boldsymbol{I} + \boldsymbol{H}\boldsymbol{S}\boldsymbol{H}^H|$$

$$\text{s.t.} \quad \text{tr}(\boldsymbol{S}) \le P, \boldsymbol{S} \succeq 0.$$

The optimal solution to the above problem is known to have the following form [13]: $\boldsymbol{S}_{\text{ID}} = \boldsymbol{V}_H \boldsymbol{\Lambda} \boldsymbol{V}_H^H$, where $\boldsymbol{V}_H \in \mathbb{C}^{M \times T_2}$ is obtained from the (reduced) SVD of $\boldsymbol{H}$ expressed by $\boldsymbol{H} = \boldsymbol{U}_H \boldsymbol{\Gamma}_H^{1/2} \boldsymbol{V}_H^H$, with $T_2 = \min(M, N_{\text{ID}})$, $\boldsymbol{U}_H \in \mathbb{C}^{N_{\text{ID}} \times T_2}$, $\boldsymbol{\Gamma}_H = \text{diag}(h_1, \ldots, h_{T_2})$, $h_1 \ge h_2 \ge \ldots \ge h_{T_2} \ge 0$, and $\boldsymbol{\Lambda} = \text{diag}(p_1, \ldots, p_{T_2})$ with the diagonal elements obtained from the standard "water-filling (WF)" power allocation solution [13]:

$$p_i = \left(\nu - \frac{1}{h_i} \right)^+, \quad i = 1, \ldots, T_2 \tag{3}$$

with ν being the so-called (constant) water-level that makes $\sum_{i=1}^{T_2} p_i = P$. The corresponding maximum transmission rate is then given by $R_{\max} = \sum_{i=1}^{T_2} \log(1 + h_i p_i)$. The maximum rate is achieved in general by *spatial multiplexing* [6] over up to T_2 spatially decoupled AWGN channels, together with the Gaussian codebook, i.e., the transmitted signal can be expressed as $\boldsymbol{x}(n) = \boldsymbol{V}_H \boldsymbol{\Lambda}^{1/2} \boldsymbol{s}(n)$, where $\boldsymbol{s}(n)$ is a Gaussian random vector $\sim \mathcal{CN}(\boldsymbol{0}, \boldsymbol{I})$, $\boldsymbol{V}_H$ and $\boldsymbol{\Lambda}^{1/2}$ denote the precoding matrix and the (diagonal) power allocation matrix, respectively.

Remark 2.1: It is worth noting that in Problem (P1), it is assumed that the transmitter sends to the EH receiver continuously. Now suppose that the transmitter only transmits a fraction of the total time denoted by α with $0 < \alpha \le 1$. Furthermore, assume that the transmit power level can be adjusted flexibly provided that the consumed average power is bounded by P, i.e., $\alpha \cdot \text{tr}(\boldsymbol{S}) + (1 - \alpha) \cdot 0 \le P$ or $\text{tr}(\boldsymbol{S}) \le P/\alpha$. In this case, it can be easily shown that the transmit covariance $\boldsymbol{S} = (P/\alpha)\boldsymbol{v}_1 \boldsymbol{v}_1^H$ also achieves the maximum harvested power $Q_{\max} = g_1 P$ for any $0 < \alpha \le 1$, which suggests that the maximum power delivered is independent of transmission time. However, unlike the case of maximum power transfer, the maximum information rate reliably transmitted to the ID receiver requires that the transmitter send signals continuously, i.e., $\alpha = 1$, as assumed in Problem (P2). This can be easily verified by observing that for any $0 < \alpha \le 1$ and $\boldsymbol{S} \succeq 0$, $\alpha \log |\boldsymbol{I} + \boldsymbol{H}(\boldsymbol{S}/\alpha)\boldsymbol{H}^H| \le \log |\boldsymbol{I} + \boldsymbol{H}\boldsymbol{S}\boldsymbol{H}^H|$ where the equality holds only when $\alpha = 1$, since R is a nonlinear concave function of $\boldsymbol{S}$. Thus, to maximize both power and rate transfer at the same time, the transmitter should broadcast to the EH and ID receivers all the time. Furthermore, note that the assumed Gaussian distribution for transmitted signals is necessary for achieving the maximum rate transfer, but not necessary for the maximum power transfer. In fact, for any arbitrary complex number c that satisfies $|c| = 1$, even a deterministic transmitted signal $\boldsymbol{x}(n) = \sqrt{P}\boldsymbol{v}_1 c, \forall n$, achieves the maximum transferred power $Q_{\max}$ in Problem (P1). However, to maximize simultaneous power and information transfer with the same transmitted signal, the Gaussian input distribution is sufficient as well as necessary.

Now, consider the case where both the EH and ID receivers are present. From the above results, it is seen that the
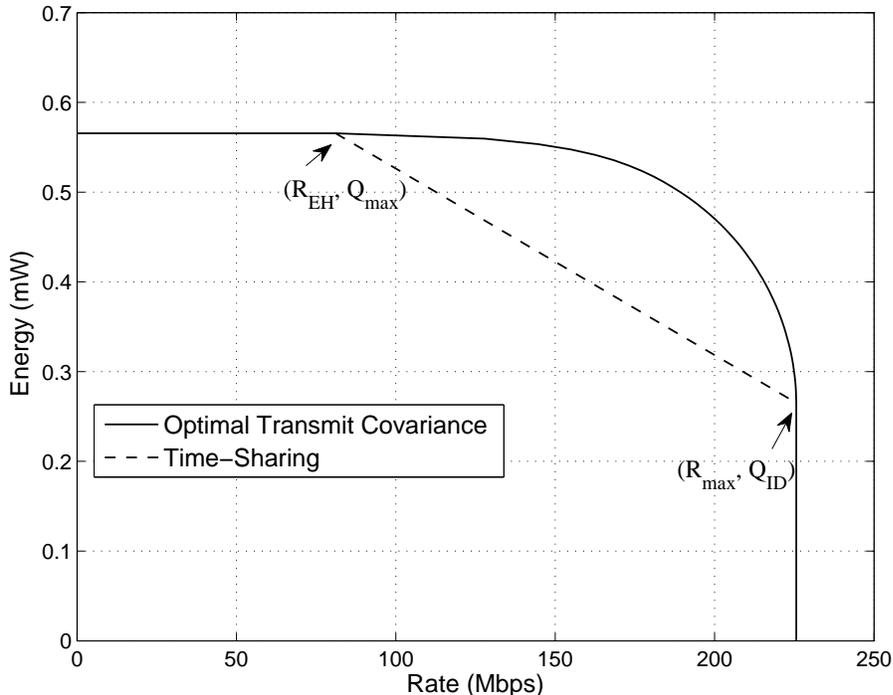
Fig. 4. Rate-energy tradeoff for a MIMO broadcast system with separated EH and ID receivers, and $M = N_{\mathrm{EH}} = N_{\mathrm{ID}} = 4$.

optimal transmission strategies for maximal power transfer and information transfer are in general different, which are energy beamforming and information spatial multiplexing, respectively. It thus motivates our investigation of the following question: What is the optimal broadcasting strategy for simultaneous wireless power and information transfer? To answer this question, we propose to use the *Rate-Energy* (R-E) region (defined below) to characterize all the achievable rate (in bits/sec/Hz or bps for information transfer) and energy (in joule/sec or watt for power transfer) pairs under a given transmit power constraint. Without loss of generality, assuming that the transmitter sends Gaussian signals continuously (cf. Remark 2.1), the R-E region is defined as

$$\mathcal{C}_{\mathrm{R-E}}(P) \triangleq \left\{ (R,Q) : R \le \log|\boldsymbol{I} + \boldsymbol{H}\boldsymbol{S}\boldsymbol{H}^H|, Q \le \mathtt{tr}(\boldsymbol{G}\boldsymbol{S}\boldsymbol{G}^H), \mathtt{tr}(\boldsymbol{S}) \le P, \boldsymbol{S} \succeq 0 \right\}. \tag{4}$$

In Fig. 4, an example of the above defined R-E region (see Section III for the algorithm to compute the boundary of this region) is shown for a practical MIMO broadcast system with separated EH and ID receivers (i.e., $\boldsymbol{G} \ne \boldsymbol{H}$). It is assumed that $M = N_{\mathrm{EH}} = N_{\mathrm{ID}} = 4$. The transmitter power is assumed to be $P = 1$ watt(W) or 30dBm. The distances from the transmitter to the EH and ID receivers are assumed to be 1 meter and 10 meters, respectively; thus, we can exploit the near-far based energy and information transmission scheduling, which may correspond to, e.g., a dedicated energy transfer system (to "near" users) with opportunistic information transmission (to "far" users), or vice versa. Assuming a carrier frequency of $f_c = 900$MHz and the power pathloss exponent to be 4, the distance-dependent signal attenuation from the AP to EH/ID receiver can be estimated as 40dB and 80dB,

respectively. Accordingly, the average signal power at the EH/ID receiver is thus $30\text{dBm}-40\text{dB}= -10\text{dBm}$ and $30\text{dBm}-80\text{dB}= -50\text{dBm}$, respectively. It is further assumed that in addition to signal pathloss, Rayleigh fading is present, as such each element of channel matrices $\boldsymbol{G}$ and $\boldsymbol{H}$ is independently drawn from the CSCG distribution with zero mean and variance -10dBm (for EH receiver) and -50dBm for (for ID receiver), respectively (to be consistent with the signal pathloss previously assumed). Furthermore, the bandwidth of the transmitted signal is assumed to be 10MHz, while the receiver noise is assumed to be white Gaussian with power spectral density -140dBm/Hz (which is dominated by the receiver processing noise rather than the background thermal noise) or average power -70dBm over the bandwidth of 10MHz. As a result, considering all of transmit power, signal attenuation, fading and receiver noise, the per-antenna average SNR at the ID receiver is equal to $30 - 80 - (-70) = 20\text{dB}$, which corresponds to $P = 100$ in the equivalent signal model for the ID receiver given in (2) with unit-norm noise. In addition, we assume that for the EH receiver, the energy conversion efficiency is $\zeta = 50\%$. Considering this together with transmit power and signal attenuation, the average per-antenna signal power at the EH receiver is thus $0.5\times(30\text{dBm}-40\text{dB}) = 50\mu\text{W}$.

From Fig. 4, it is observed that with energy beamforming, the maximum harvested energy rate for the EH receiver is around $Q_{\text{max}} = 0.57\text{mW}$, while with spatial multiplexing, the maximum information rate for the ID receiver is around $R_{\text{max}} = 225\text{Mbps}$. It is easy to identify two boundary points of this R-E region denoted by $(R_{\text{EH}}, Q_{\text{max}})$ and $(R_{\text{max}}, Q_{\text{ID}})$, respectively. For the former boundary point, the transmit covariance is $\boldsymbol{S}_{\text{EH}}$, which corresponds to transmit beamforming and achieves the maximum transferred power Q_{max} to the EH receiver, while the resulting information rate for the ID receiver is given by $R_{\text{EH}} = \log(1 + \|\boldsymbol{H}\boldsymbol{v}_1\|^2 P)$. On the other hand, for the latter boundary point, the transmit covariance is $\boldsymbol{S}_{\text{ID}}$, which corresponds to transmit spatial multiplexing and achieves the maximum information rate transferred to the ID receiver R_{max}, while the resulting power transferred to the EH receiver is given by $Q_{\text{ID}} = \text{tr}(\boldsymbol{G}\boldsymbol{S}_{\text{ID}}\boldsymbol{G}^H)$.

Since the optimal tradeoff between the maximum energy and information transfer rates is characterized by the boundary of the R-E region, it is important to characterize all the boundary rate-power pairs of $\mathcal{C}_{\text{R}-\text{E}}(P)$ for any $P > 0$. From Fig. 4, it is easy to observe that if $R \leq R_{\text{EH}}$, the maximum harvested power Q_{max} is achievable with the same transmit covariance that achieves the rate-power pair $(R_{\text{EH}}, Q_{\text{max}})$; similarly, the maximum information rate R_{max} is achievable provided that $Q \leq Q_{\text{ID}}$. Thus, the remaining boundary of $\mathcal{C}_{\text{R}-\text{E}}(P)$ yet to be characterized is over the intervals: $R_{\text{EH}} < R < R_{\text{max}}$, $Q_{\text{ID}} < Q < Q_{\text{max}}$. We thus consider the following optimization problem:

$$\text{(P3)} \quad \max_{\boldsymbol{S}} \quad \log\left|\boldsymbol{I} + \boldsymbol{H}\boldsymbol{S}\boldsymbol{H}^H\right|$$

$$\text{s.t.} \quad \text{tr}\left(\boldsymbol{G}\boldsymbol{S}\boldsymbol{G}^H\right) \geq \bar{Q}, \ \text{tr}(\boldsymbol{S}) \leq P, \ \boldsymbol{S} \succeq 0.$$

Note that if $\bar{Q}$ takes values from $Q_{\text{ID}} < \bar{Q} < Q_{\text{max}}$, the corresponding optimal rate solutions of the above problems

are the boundary rate points of the R-E region over $R_{\mathrm{EH}} < R < R_{\max}$. Notice that the transmit covariance solutions to the above problems in general yield larger rate-power pairs than those by simply "time-sharing" the optimal transmit covariance matrices $\boldsymbol{S}_{\mathrm{EH}}$ and $\boldsymbol{S}_{\mathrm{ID}}$ for EH and ID receivers separately (see the dashed line in Fig. 4).[3]

Problem (P3) is a convex optimization problem, since its objective function is concave over $\boldsymbol{S}$ and its constraints specify a convex set of $\boldsymbol{S}$. Note that (P3) resembles a similar problem formulated in [15], [16] (see also [17] and references therein) under the cognitive radio (CR) setup, where the rate of a secondary MIMO link is maximized subject to a set of so-called *interference power constraints* to protect the co-channel primary receivers. However, there is a key difference between (P3) and the problem in [16]: the harvested power constraint in (P3) has the reversed inequality of that of the interference power constraint in [16], since in our case it is desirable for the EH receiver to harvest more power from the transmitter, as opposed to that in [16] the interference power at the primary receiver should be minimized. As such, it is not immediately clear whether the solution in [16] can be directly applied for solving (P3) with the reversed power inequality. In the following, we will examine the solutions to Problem (P3) for the two cases with arbitrary $\boldsymbol{G}$ and $\boldsymbol{H}$ (the case of separated receivers) and $\boldsymbol{G} = \boldsymbol{H}$ (the case of co-located receivers), respectively.

III. SEPARATED RECEIVERS

Consider the case where the EH receiver and ID receiver are spatially separated and thus in general have different channels from the transmitter. In this section, we first solve Problem (P3) with arbitrary $\boldsymbol{G}$ and $\boldsymbol{H}$ and derive a semi-closed-form expression for the optimal transmit covariance. Then, we examine the optimal solution for the special case of MISO channels from the transmitter to ID and/or EH receivers.

Since Problem (P3) is convex and satisfies the Slater's condition [18], it has a zero duality gap and thus can be solved using the Lagrange duality method.[4] Thus, we introduce two non-negative dual variables, λ and μ, associated with the harvested power constraint and transmit power constraint in (P3), respectively. The optimal solution to Problem (P3) is then given by the following theorem in terms of λ^* and μ^*, which are the optimal dual solutions of Problem (P3) (see Appendix B for details). Note that for Problem (P3), given any pair of $\bar{Q}$ ($Q_{\mathrm{ID}} < \bar{Q} < Q_{\max}$) and $P > 0$, there exists one unique pair of $\lambda^* > 0$ and $\mu^* > 0$.

Theorem 3.1: The optimal solution to Problem (P3) has the following form:

$$\boldsymbol{S}^* = \boldsymbol{A}^{-1/2}\tilde{\boldsymbol{V}}\tilde{\boldsymbol{\Lambda}}\tilde{\boldsymbol{V}}^H\boldsymbol{A}^{-1/2} \tag{5}$$

---

[3]By time-sharing, we mean that the AP transmits simultaneously to both EH and ID receivers with the energy-maximizing transmit covariance $\boldsymbol{S}_{\mathrm{EH}}$ (i.e. energy beamforming) for β portion of each block time, and the information-rate-maximizing transmit covariance $\boldsymbol{S}_{\mathrm{ID}}$ (i.e. spatial multiplexing) for the remaining $1 - \beta$ portion of each block time, with $0 \leq \beta \leq 1$.

[4]It is worth noting that Problem (P3) is convex and thus can be solved efficiently by the interior point method [18]; in this paper, we apply the Lagrange duality method for this problem mainly to reveal the optimal precoder structure.

where $\boldsymbol{A} = \mu^*\boldsymbol{I} - \lambda^*\boldsymbol{G}^H\boldsymbol{G}$, $\tilde{\boldsymbol{V}} \in \mathbb{C}^{M \times T_2}$ is obtained from the (reduced) SVD of the matrix $\boldsymbol{H}\boldsymbol{A}^{-1/2}$ given by $\boldsymbol{H}\boldsymbol{A}^{-1/2} = \tilde{\boldsymbol{U}}\tilde{\boldsymbol{\Gamma}}^{1/2}\tilde{\boldsymbol{V}}^H$, with $\tilde{\boldsymbol{\Gamma}} = \mathtt{diag}(\tilde{h}_1, \ldots, \tilde{h}_{T_2})$, $\tilde{h}_1 \geq \tilde{h}_2 \geq \ldots \geq \tilde{h}_{T_2} \geq 0$, and $\tilde{\boldsymbol{\Lambda}} = \mathtt{diag}(\tilde{p}_1, \ldots, \tilde{p}_{T_2})$, with $\tilde{p}_i = (1 - 1/\tilde{h}_i)^+, i = 1, \ldots, T_2$.

Proof: See Appendix B. ∎

Note that this theorem requires that $\boldsymbol{A} = \mu^*\boldsymbol{I} - \lambda^*\boldsymbol{G}^H\boldsymbol{G} \succ 0$, implying that $\mu^* > \lambda^*g_1$ (recall that g_1 is the largest eigenvalue of matrix $\boldsymbol{G}^H\boldsymbol{G}$), which is not present for a similar result in [17] under the CR setup with the reversed interference power constraint. One algorithm that can be used to solve (P3) is provided in Table I of Appendix B. From Theorem 3.1, the maximum transmission rate for Problem (P3) can be shown to be $R^* = \log\left|\boldsymbol{I} + \boldsymbol{H}\boldsymbol{S}^*\boldsymbol{H}^H\right| = \sum_{i=1}^{T_2}\log(1 + \tilde{h}_i\tilde{p}_i)$, for which the proof is omitted here for brevity.

Next, we examine the optimal solution to Problem (P3) for the special case where the ID receiver has one single antenna, i.e., $N_{\mathrm{ID}} = 1$, and thus the MIMO channel $\boldsymbol{H}$ reduces to a row vector $\boldsymbol{h}^H$ with $\boldsymbol{h} \in \mathbb{C}^{M \times 1}$. Suppose that the EH receiver is still equipped with $N_{\mathrm{EH}} \geq 1$ antennas, and thus the MIMO channel $\boldsymbol{G}$ remains unchanged. From Theorem 3.1, we obtain the following corollary.

Corollary 3.1: In the case of MISO channel from the transmitter to ID receiver, i.e., $\boldsymbol{H} \equiv \boldsymbol{h}^H$, the optimal solution to Problem (P3) reduces to the following form:

$$\boldsymbol{S}^* = \boldsymbol{A}^{-1}\boldsymbol{h}\left(\frac{1}{\|\boldsymbol{A}^{-1/2}\boldsymbol{h}\|^2} - \frac{1}{\|\boldsymbol{A}^{-1/2}\boldsymbol{h}\|^4}\right)^+\boldsymbol{h}^H\boldsymbol{A}^{-1} \tag{6}$$

where $\boldsymbol{A} = \mu^*\boldsymbol{I} - \lambda^*\boldsymbol{G}^H\boldsymbol{G}$, with λ^* and μ^* denoting the optimal dual solutions of Problem (P3). Correspondingly, the optimal value of (P3) is $R^* = \left(2\log\left(\|\boldsymbol{A}^{-1/2}\boldsymbol{h}\|\right)\right)^+$.

Proof: See Appendix C. ∎

From (6), it is observed that the optimal transmit covariance is a *rank-one* matrix, from which it follows that *beamforming* is the optimal transmission strategy in this case, where the transmit beamforming vector should be aligned with the vector $\boldsymbol{A}^{-1}\boldsymbol{h}$. Moreover, consider the case where both channels from the transmitter to ID/EH receivers are MISO, i.e., $\boldsymbol{H} \equiv \boldsymbol{h}^H$, and $\boldsymbol{G} \equiv \boldsymbol{g}^H$ with $\boldsymbol{g} \in \mathbb{C}^{M \times 1}$. From Corollary 3.1, it follows immediately that the optimal covariance solution to Problem (P3) is still beamforming. In the following theorem, we show a closed-form solution of the optimal beamforming vector at the transmitter for this special case, which differs from the semi-closed-form solution (6) that was expressed in terms of dual variables.

<u>Theorem 3.2</u>: In the case of MISO channels from transmitter to both ID and EH receivers, i.e., $\boldsymbol{H} \equiv \boldsymbol{h}^H$, and $\boldsymbol{G} \equiv \boldsymbol{g}^H$, the optimal solution to Problem (P3) can be expressed as $\boldsymbol{S}^* = P\boldsymbol{v}\boldsymbol{v}^H$, where the beamforming vector $\boldsymbol{v}$ has a unit-norm and is given by

$$\boldsymbol{v} = \begin{cases} \hat{\boldsymbol{h}} & 0 \leq \bar{Q} \leq |\boldsymbol{g}^H\hat{\boldsymbol{h}}|^2P \\ \sqrt{\frac{\bar{Q}}{P\|\boldsymbol{g}\|^2}}e^{j\angle\alpha_{gh}}\hat{\boldsymbol{g}} + \sqrt{1 - \frac{\bar{Q}}{P\|\boldsymbol{g}\|^2}}\hat{\boldsymbol{h}}_{g^\perp} & |\boldsymbol{g}^H\hat{\boldsymbol{h}}|^2P < \bar{Q} \leq P\|\boldsymbol{g}\|^2 \end{cases} \tag{7}$$
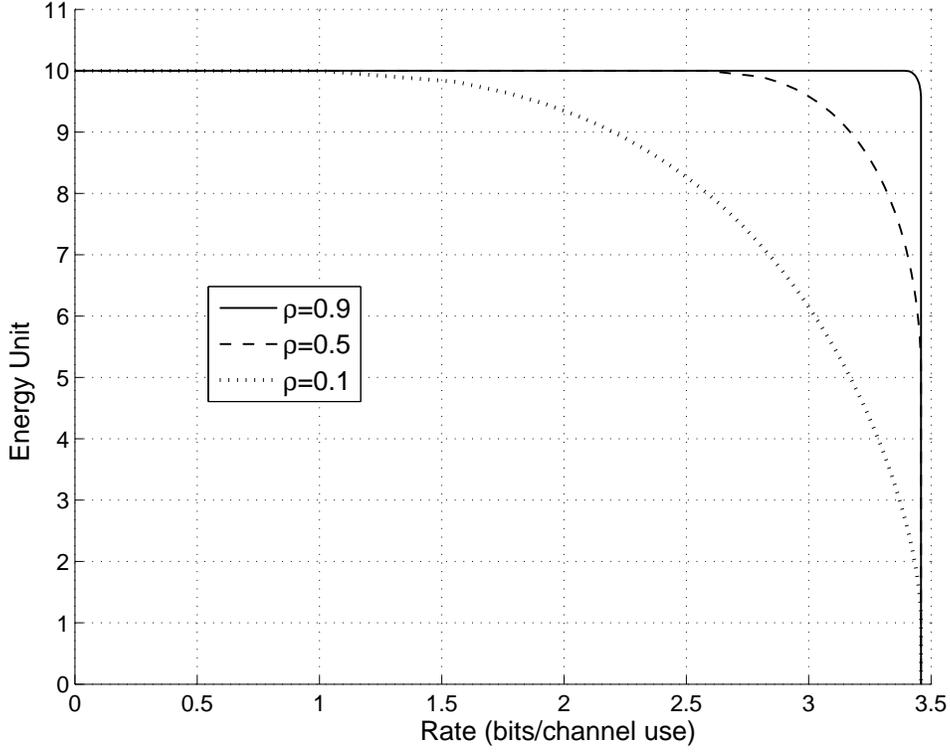
Fig. 5. Rate-energy tradeoff for a MISO broadcast system with correlated MISO channels to the (separated) EH and ID receivers.

where $\hat{\boldsymbol{h}} = \boldsymbol{h}/\|\boldsymbol{h}\|$, $\hat{\boldsymbol{g}} = \boldsymbol{g}/\|\boldsymbol{g}\|$, $\hat{\boldsymbol{h}}_{g^\perp} = \boldsymbol{h}_{g^\perp}/\|\boldsymbol{h}_{g^\perp}\|$ with $\boldsymbol{h}_{g^\perp} = \boldsymbol{h} - (\hat{\boldsymbol{g}}^H \boldsymbol{h})\hat{\boldsymbol{g}}$, and $\alpha_{gh} = \hat{\boldsymbol{g}}^H \boldsymbol{h}$ with $\angle\alpha_{gh} \in [0, 2\pi)$ denoting the phase of complex number α_{gh}. Correspondingly, the optimal value of (P3) is given by

$$R^* = \begin{cases} \log(1 + \|\boldsymbol{h}\|^2 P) & 0 \leq \bar{Q} \leq |\boldsymbol{g}^H\hat{\boldsymbol{h}}|^2 P \\ \log\left(1 + \left(\sqrt{\frac{\bar{Q}}{\|\boldsymbol{g}\|^2}}|\alpha_{gh}| + \sqrt{P - \frac{\bar{Q}}{\|\boldsymbol{g}\|^2}}\sqrt{\|\boldsymbol{h}\|^2 - |\alpha_{gh}|^2}\right)^2\right) & |\boldsymbol{g}^H\hat{\boldsymbol{h}}|^2 P < \bar{Q} \leq P\|\boldsymbol{g}\|^2. \end{cases} \quad (8)$$

Proof: The proof is similar to that of Theorem 2 in [16], and is thus omitted for brevity. ∎

It is worth noting that in (7), if $\bar{Q} \leq |\boldsymbol{g}^H\hat{\boldsymbol{h}}|^2 P$, the optimal transmit beamforming vector is based on the principle of maximal-ratio-combining (MRC) with respect to the MISO channel $\boldsymbol{h}^H$ from the transmitter to the ID receiver, and in this case, the harvested power constraint in Problem (P3) is indeed not active; however, when $\bar{Q} > |\boldsymbol{g}^H\hat{\boldsymbol{h}}|^2 P$, the optimal beamforming vector is a linear combination of the two vectors $\hat{\boldsymbol{g}}$ and $\hat{\boldsymbol{h}}_{g^\perp}$, and the combining coefficients are designed such that the harvested power constraint is satisfied with equality.

In Fig. 5, we show the achievable R-E regions for the case of MISO channels from the transmitter to both EH and ID receivers. We set $P = 10$. For the purpose of exposition, it is assumed that $\|\boldsymbol{h}\| = \|\boldsymbol{g}\| = 1$ and $|\alpha_{gh}|^2 = \rho$, with $0 \leq \rho \leq 1$ denoting the correlation between the two unit-norm vectors $\boldsymbol{h}$ and $\boldsymbol{g}$. This channel setup may correspond to the practical scenario where the EH and ID receivers are equipped at a single device (but still physically separated), and as a result their respective MISO channels from the transmitter have the same power gain but are spatially correlated due to the insufficient spacing between two separate receiving antennas. From Theorem 3.2, the R-E regions for the three cases of $\rho = 0.1, 0.5$, and 0.9 are obtained, as shown in Fig. 5.

Interestingly, it is observed that increasing ρ enlarges the achievable R-E region, which indicates that the antenna correlation between the EH and ID receivers can be a beneficial factor for simultaneous information and power transfer. Note that in this figure, we express energy and rate in terms of energy unit and bits/channel use, respectively, since their practical values can be obtained by appropriate scaling based on the realistic system parameters as for Fig. 4.

IV. CO-LOCATED RECEIVERS

In this section, we address the case where the EH and ID receivers are co-located, and thus possess the same channel from the transmitter, i.e., $G = H$ and thus $N_{\text{EH}} = N_{\text{ID}} \triangleq N$. We first examine the optimal solution of Problem (P3) for this case, from which we obtain an outer bound for the achievable rate-power pairs in the R-E region. Then, we propose two practical receiver designs, namely time switching and power splitting, derive their optimal transmission strategies to maximize the achievable rate-power pairs, and finally compare the results to the R-E region outer bound.

A. Performance Outer Bound

Consider Problem (P3) with $G = H$. Recall that the (reduced) SVD of H is given by $H = U_H \Gamma_H^{1/2} V_H^H$, with $\Gamma_H = \text{diag}(h_1, \ldots, h_{T_2})$, $h_1 \geq h_2 \geq \ldots \geq h_{T_2} \geq 0$, and $T_2 = \min(M, N)$. From Theorem 3.1, we obtain the following corollary.

Corollary 4.1: In the case of co-located EH and ID receivers with $G = H$, the optimal solution to Problem (P3) has the form of $S^* = V_H \Sigma V_H^H$, where $\Sigma = \text{diag}(\hat{p}_1, \ldots, \hat{p}_{T_2})$ with the diagonal elements obtained from the following modified WF power allocation:

$$\hat{p}_i = \left(\frac{1}{\mu^* - \lambda^* h_i} - \frac{1}{h_i} \right)^+, \quad i = 1, \ldots, T_2 \tag{9}$$

with λ^* and μ^* denoting the optimal dual solutions of Problem (P3), $\mu^* > \lambda^* h_1$. The corresponding maximum transmission rate is $R^* = \sum_{i=1}^{T_2} \log(1 + h_i \hat{p}_i)$.

Proof: See Appendix D. ∎

The algorithm in Table I for solving Problem (P3) with arbitrary G and H can be simplified to solve the special case with $G = H$. Corollary 4.1 reveals that for Problem (P3) in the case of $G = H$, the optimal transmission strategy is in general still spatial multiplexing over the eigenmodes of the MIMO channel H as for Problem (P2), while the optimal tradeoffs between information transfer and power transfer are achieved by varying the power levels allocated into different eigenmodes, as shown in (9). It is interesting to observe that the power allocation in (9) reduces to the conventional WF solution in (3) with a constant water-level when $\lambda^* = 0$, i.e., the harvested power constraint in Problem (P3) is inactive with the optimal power allocation. However, when $\lambda^* > 0$ and thus

the harvested power constraint is active corresponding to the Pareto-optimal regime of our interest, the power allocation in (9) is observed to have a *non-decreasing* water-level as h_i's increase. Note that this modified WF policy has also been shown in [2] for power allocation in frequency-selective AWGN channels.

Using Corollary 4.1, we can characterize all the boundary points of the R-E region $\mathcal{C}_{\mathrm{R-E}}(P)$ defined in (4) for the case of co-located receivers with $\boldsymbol{G} = \boldsymbol{H}$. For example, if the total transmit power is allocated to the channel with the largest gain h_1, i.e., $\hat{p}_1 = P$ and $\hat{p}_i = 0, i = 2, \ldots, T_2$, the maximum harvested power $Q_{\mathrm{max}} = P h_1$ is achieved by transmit beamforming. On the other hand, if transmit spatial multiplexing is applied with the conventional WF power allocation given in (9) with $\lambda^* = 0$, the corresponding R^* becomes the maximum transmission rate, R_{max}. However, unlike the case of separated EH and ID receivers in which the entire boundary of $\mathcal{C}_{\mathrm{R-E}}(P)$ is achievable, in the case of co-located receivers, except the two boundary rate-power pairs $(R_{\mathrm{max}}, 0)$ and $(0, Q_{\mathrm{max}})$, all the other boundary pairs of $\mathcal{C}_{\mathrm{R-E}}(P)$ may not be achievable in practice. Note that these boundary points are achievable if and only if (iff) the following premise is true: the power of the received signal across all antennas is totally harvested, and at the same time the carried information with a transmission rate up to the MIMO channel capacity (for a given transmit covariance) is decodable. However, existing EH circuits are not yet able to directly decode the information carried in the RF-band signal, even for the SISO channel case; as a result, how to achieve the remaining boundary rate-power pairs of $\mathcal{C}_{\mathrm{R-E}}(P)$ in the MIMO case with the co-located EH and ID receiver remains an interesting open problem. Therefore, in the case of co-located receivers, the boundary of $\mathcal{C}_{\mathrm{R-E}}(P)$ given by Corollary 4.1 in general only serves as an *outer bound* for the achievable rate-power pairs with practical receiver designs, as will be investigated in the following subsections.

B. Time Switching

First, as shown in Fig. 3(a), we consider the *time switching* (TS) scheme, with which each transmission block is divided into two orthogonal time slots, one for transferring power and the other for transmitting data. The co-located EH and ID receiver switches its operations periodically between harvesting energy and decoding information between the two time slots. It is assumed that time synchronization has been perfectly established between the transmitter and the receiver, and thus the receiver can synchronize its function switching with the transmitter. With orthogonal transmissions, the transmitted signals for the EH receiver and ID receiver can be designed separately, but subject to a total transmit power constraint. Let α with $0 \leq \alpha \leq 1$ denote the percentage of transmission time allocated to the EH time slot. We then consider the following two types of power constraints at the transmitter:

- *Fixed power constraint*: The transmitted signals to the ID and EH receivers have the same fixed power constraint given by $\mathrm{tr}(\boldsymbol{S}_1) \leq P$, and $\mathrm{tr}(\boldsymbol{S}_2) \leq P$, where $\boldsymbol{S}_1$ and $\boldsymbol{S}_2$ denote the transmit covariance matrices for the ID and EH transmission time slots, respectively.

- *Flexible power constraint*: The transmitted signals to the ID and EH receivers can have different power constraints provided that their average consumed power is below P, i.e., $(1-\alpha)\text{tr}(\boldsymbol{S}_1) + \alpha\text{tr}(\boldsymbol{S}_2) \le P$.

Note that the TS scheme under the fixed power constraint has been considered in [14] for the single-antenna AWGN channel. The achievable R-E regions for the TS scheme with the fixed (referred to as TS_1) vs. flexible (referred to as TS_2) power constraints are then given as follows:

$$\mathcal{C}_{\text{R-E}}^{\text{TS}_1}(P) \triangleq \bigcup_{0 \le \alpha \le 1} \left\{ (R,Q) : R \le (1-\alpha)\log|\boldsymbol{I} + \boldsymbol{H}\boldsymbol{S}_1\boldsymbol{H}^H|, \right.$$
$$\left. Q \le \alpha\text{tr}(\boldsymbol{H}\boldsymbol{S}_2\boldsymbol{H}^H), \text{tr}(\boldsymbol{S}_1) \le P, \text{tr}(\boldsymbol{S}_2) \le P \right\} \tag{10}$$

$$\mathcal{C}_{\text{R-E}}^{\text{TS}_2}(P) \triangleq \bigcup_{0 \le \alpha \le 1} \left\{ (R,Q) : R \le (1-\alpha)\log|\boldsymbol{I} + \boldsymbol{H}\boldsymbol{S}_1\boldsymbol{H}^H|, \right.$$
$$\left. Q \le \alpha\text{tr}(\boldsymbol{H}\boldsymbol{S}_2\boldsymbol{H}^H), (1-\alpha)\text{tr}(\boldsymbol{S}_1) + \alpha\text{tr}(\boldsymbol{S}_2) \le P \right\}. \tag{11}$$

It is worth noting that $\mathcal{C}_{\text{R-E}}^{\text{TS}_1}(P) \subseteq \mathcal{C}_{\text{R-E}}^{\text{TS}_2}(P)$ must be true since any pair of $\boldsymbol{S}_1 \succeq 0$ and $\boldsymbol{S}_2 \succeq 0$ that satisfy the fixed power constraint will satisfy the flexible power constraint, but not vice versa. The optimal transmit covariance matrices $\boldsymbol{S}_1$ and $\boldsymbol{S}_2$ to achieve the boundary of $\mathcal{C}_{\text{R-E}}^{\text{TS}_1}(P)$ with the fixed power constraint are given in Section II (assuming $\boldsymbol{G} = \boldsymbol{H}$). In fact, the boundary of $\mathcal{C}_{\text{R-E}}^{\text{TS}_1}(P)$ is simply a straight line connecting the two points $(R_{\max}, 0)$ and $(0, Q_{\max})$ (cf. Fig. 7) by sweeping α from 0 to 1.

Similarly, for the case of flexible power constraint, the transmit covariance solutions for $\boldsymbol{S}_1$ and $\boldsymbol{S}_2$ to achieve any boundary point of $\mathcal{C}_{\text{R-E}}^{\text{TS}_2}(P)$ can be shown to have the same set of eigenvectors as those given in Section II (assuming $\boldsymbol{G} = \boldsymbol{H}$), respectively; however, the corresponding time allocation for α and power allocation for $\boldsymbol{S}_1$ and $\boldsymbol{S}_2$ remain unknown. We thus have the following proposition.

Proposition 4.1: In the case of flexible power constraint, except the two points $(R_{\max}, 0)$ and $(0, Q_{\max})$, all other boundary points of the region $\mathcal{C}_{\text{R-E}}^{\text{TS}_2}(P)$ are achieved as $\alpha \to 0$; accordingly, $\mathcal{C}_{\text{R-E}}^{\text{TS}_2}(P)$ can be simplified as

$$\mathcal{C}_{\text{R-E}}^{\text{TS}_2}(P) = \left\{ (R,Q) : R \le \log|\boldsymbol{I} + \boldsymbol{H}\boldsymbol{S}_1\boldsymbol{H}^H|, \text{tr}(\boldsymbol{S}_1) \le (P - Q/h_1), \boldsymbol{S}_1 \succeq 0 \right\}. \tag{12}$$

Proof: See Appendix E. ∎

The corresponding optimal power allocation for $\boldsymbol{S}_1$ and $\boldsymbol{S}_2$ can be easily obtained given (12) and are thus omitted for brevity. Proposition 4.1 suggests that to achieve any boundary point (R,Q) of $\mathcal{C}_{\text{R-E}}^{\text{TS}_2}(P)$ with $R < R_{\max}$ and $Q < Q_{\max}$, the portion of transmission time α allocated to power transfer in each block should asymptotically go to zero when $n \to \infty$, where n denotes the number of transmitted symbols in each block. For example, by allocating $O(\log n)$ symbols per block for power transfer and the remaining symbols for information transmission yields $\alpha = \log n / n \to 0$ as $n \to \infty$, which satisfies the optimality condition given in Proposition 4.1.
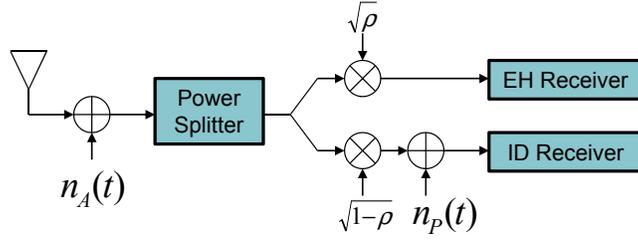
(a) Co-located receivers with a power splitter
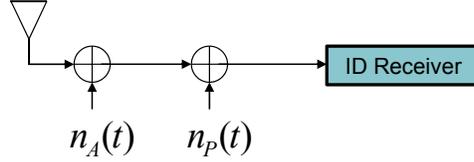
(b) ID receiver without a power splitter

Fig. 6.   Receiver operations with/without a power splitter (the energy harvested due to the receiver noise is ignored for EH receiver).

It is worth noting that the boundary of $\mathcal{C}_{\mathrm{R-E}}^{\mathrm{TS}_2}(P)$ in the flexible power constraint case is achieved under the assumption that the transmitter and receiver can both operate in the regime of infinite power in the EH time slot due to $\alpha \to 0$, which cannot be implemented with practical power amplifiers. Hence, a more feasible region for $\mathcal{C}_{\mathrm{R-E}}^{\mathrm{TS}_2}(P)$ is obtained by adding peak[5] transmit power constraints in (11) as $\mathtt{tr}(\boldsymbol{S}_1) \leq P_{\mathrm{peak}}$ and $\mathtt{tr}(\boldsymbol{S}_2) \leq P_{\mathrm{peak}}$, with $P_{\mathrm{peak}} \geq P$. Similar to Proposition 4.1, it can be shown that the boundary of the achievable R-E region in this case, denoted by $\mathcal{C}_{\mathrm{R-E}}^{\mathrm{TS}_2}(P, P_{\mathrm{peak}})$, is achieved by $\alpha = Q/(h_1 P_{\mathrm{peak}})$. Note that we can equivalently denote the achievable R-E region $\mathcal{C}_{\mathrm{R-E}}^{\mathrm{TS}_2}(P)$ defined in (11) or (12) without any peak power constraint as $\mathcal{C}_{\mathrm{R-E}}^{\mathrm{TS}_2}(P, \infty)$.

C. Power Splitting

Next, we propose an alternative receiver design called *power splitting* (PS), whereby the power and information transfer to the co-located EH and ID receivers are simultaneously achieved via a set of power splitting devices, one device for each receiving antenna, as shown in Fig. 3(b). In order to gain more insight into the PS scheme, we consider first the simple case of a single-antenna AWGN channel with co-located ID and EH receivers, which is shown in Fig. 6(a). For the ease of comparison, the case of solely information transfer with one single ID receiver is also shown in Fig. 6(b).

The receiver operations in Fig. 6(a) are explained as follows: The received signal from the antenna is first corrupted by a Gaussian noise denoted by $n_A(t)$ at the RF-band, which is assumed to have zero mean and equivalent baseband power σ_A^2. The RF-band signal is then fed into a power splitter, which is assumed to be perfect without any noise induced. After the power splitter, the portion of signal power split to the EH receiver is

---

[5]Note that the peak power constraint in this context is different from the signal amplitude constraint considered in [1], [14].

denoted by ρ, and that to the ID receiver by $1 - \rho$. The signal split to the ID receiver then goes through a sequence of standard operations (see, e.g., [19]) to be converted from the RF band to baseband. During this process, the signal is additionally corrupted by another noise $n_P(t)$, which is independent of $n_A(t)$ and assumed to be Gaussian and have zero mean and variance σ_P^2. To be consistent to the case with solely the ID receiver, it is reasonable to assume that the antenna noise $n_A(t)$ and processing noise $n_P(t)$ have the same distributions in both Figs. 6(a) and 6(b). It is further assumed that $\sigma_A^2 + \sigma_P^2 = 1$ to be consistent with the system model introduced in Section II.

For this simple SISO AWGN channel, we denote the transmit power constraint by P and the channel power gain by h. It is then easy to compute the R-E region outer bound $\mathcal{C}_{R-E}(P)$ for this channel with co-located ID and EH receivers, which is simply a box specified by three vertices $(0, Q_{\max})$, $(R_{\max}, 0)$ and $(R_{\max}, Q_{\max})$, with $Q_{\max} = Ph$ and $R_{\max} = \log(1 + Ph)$. Interestingly, we will show next that under certain conditions, the PS scheme can in fact achieve all the rate-energy pairs in this R-E region outer bound; without loss of generality, it suffices to show that the vertex point $(R_{\max}, Q_{\max})$ is achievable.

With reference to Fig. 6(a), we discuss the PS scheme in the following three regimes with different values of antenna and processing noise power.

- $\sigma_A^2 \ll \sigma_P^2$ (Case I): In this ideal case with perfect receiving antenna, the antenna noise can be ignored and thus we have $\sigma_A^2 = 0$ and $\sigma_P^2 = 1$. Accordingly, it is easy to show that the SNR, denoted by τ, at the ID receiver in Fig. 6(a) is $(1 - \rho)Ph$. The achievable R-E region in this case is then given by $\mathcal{C}_{R-E}^{PS,I}(P) \triangleq \bigcup_{0 \le \rho \le 1}\{(R, Q) : R \le \log(1 + (1 - \rho)Ph), Q \le \rho Ph\}$. This region can be shown to coincide with the R-E region for the TS scheme with the flexible power constraint given by (12) for the SISO case.

- $0 < \sigma_A^2 < 1$ (Case II): This is the most practically valid case. Since $\sigma_P^2 = 1 - \sigma_A^2$, we can show that τ in this case is given by $\tau = (1 - \rho)Ph/((1 - \rho)\sigma_A^2 + \sigma_P^2) = (1 - \rho)Ph/(1 - \rho\sigma_A^2)$. Accordingly, the achievable R-E region in this case is given by $\mathcal{C}_{R-E}^{PS,II}(P) \triangleq \bigcup_{0 \le \rho \le 1}\{(R, Q) : R \le \log(1 + \tau), Q \le \rho Ph\}$. It is easy to show that $\mathcal{C}_{R-E}^{PS,II}(P)$ enlarges strictly as σ_A^2 increases from 0 to 1.

- $\sigma_A^2 \gg \sigma_P^2$ (Case III): In this ideal case with perfect RF-to-baseband signal conversion, the processing noise can be ignored and thus we have $\sigma_P^2 = 0$ and $\sigma_A^2 = 1$. In this case, the SNR for the ID receiver is given by $\tau = Ph$, regardless of the value of ρ. Thus, to maximize the power transfer, ideally we should set $\rho \to 1$, i.e., splitting infinitesimally small power to the ID receiver since both the signal and antenna noise are scaled identically by the power splitter and there is no additional processing noise induced after the power splitting. With $\rho = 1$, the achievable R-E region in this case is given by $\mathcal{C}_{R-E}^{PS,III}(P) \triangleq \{(R, Q) : R \le \log(1 + Ph), Q \le Ph\}$, which becomes identical to the R-E region outer bound $\mathcal{C}_{R-E}(P)$ (which is a box as defined earlier).

Therefore, we know from the above discussions that only for the case of noise-free RF-band to baseband

processing (i.e., Case III), the PS scheme achieves the R-E region outer bound and is thus optimal. However, in practice, such a condition can never be met perfectly, and thus the R-E region outer bound $\mathcal{C}_{\mathrm{R-E}}(P)$ is in general still non-achievable with practical PS receivers. In the following, we will study further the achievable R-E region by the PS scheme for the more general case of MIMO channels. It is not difficult to show that if each receiving antenna satisfies the condition in Case III, the R-E region outer bound $\mathcal{C}_{\mathrm{R-E}}(P)$ defined in (4) with $\boldsymbol{G} = \boldsymbol{H}$ is achievable for the MIMO case by the PS scheme (with each receiving antenna to set $\rho = 1$). For a more practical purpose, we consider in the rest of this section the "worst" case performance of the PS scheme (i.e., Case I in the above), when the noiseless antenna is assumed (which leads to the smallest R-E region for the SISO AWGN channel case). The obtained R-E region will thus provide the performance lower bound for the PS scheme with practical receiver circuits. In this case, since there is no antenna noise and the processing noise is added after the power splitting, it is equivalent to assume that the aggregated receiver noise power remains unchanged with a power splitter at each receiving antenna. Let ρ_i with $0 \leq \rho_i \leq 1$ denote the portion of power split to the EH receiver at the ith receiving antenna, $1 \leq i \leq N$. The achievable R-E region for the PS scheme (in the worst case) is thus given by

$$\mathcal{C}_{\mathrm{R-E}}^{\mathrm{PS}}(P) \triangleq \bigcup_{0 \leq \rho_i \leq 1, \forall i} \left\{ (R, Q) : R \leq \log |\boldsymbol{I} + \bar{\boldsymbol{\Lambda}}_\rho^{1/2} \boldsymbol{H} \boldsymbol{S} \boldsymbol{H}^H \bar{\boldsymbol{\Lambda}}_\rho^{1/2}|, Q \leq \mathtt{tr}(\boldsymbol{\Lambda}_\rho \boldsymbol{H} \boldsymbol{S} \boldsymbol{H}^H), \mathtt{tr}(\boldsymbol{S}) \leq P, \boldsymbol{S} \succeq 0 \right\}$$

(13)

where $\boldsymbol{\Lambda}_\rho = \mathtt{diag}(\rho_1, \ldots, \rho_N)$, and $\bar{\boldsymbol{\Lambda}}_\rho = \boldsymbol{I} - \boldsymbol{\Lambda}_\rho$.

Note that the two points $(R_{\max}, 0)$ and $(0, Q_{\max})$ on the boundary of $\mathcal{C}_{\mathrm{R-E}}^{\mathrm{PS}}(P)$ can be simply achieved with $\rho_i = 0, \forall i$, and $\rho_i = 1, \forall i$, respectively, with the corresponding transmit covariance matrices given in Section II (with $\boldsymbol{G} = \boldsymbol{H}$), similar to the TS case. All the other boundary points of $\mathcal{C}_{\mathrm{R-E}}^{\mathrm{PS}}(P)$ can be obtained as follows: Let $\boldsymbol{H}' = \bar{\boldsymbol{\Lambda}}_\rho^{1/2} \boldsymbol{H}$, $\boldsymbol{G}' = \boldsymbol{\Lambda}_\rho^{1/2} \boldsymbol{H}$, and $\mathcal{R}_{\mathrm{R-E}}^{\mathrm{PS}}(P, \{\rho_i\})$ denote the achievable R-E region with PS for a given set of ρ_i's. Then, we can obtain the boundary of $\mathcal{R}_{\mathrm{R-E}}^{\mathrm{PS}}(P, \{\rho_i\})$ by solving similar problems like Problem (P3) (with $\boldsymbol{H}$ and $\boldsymbol{G}$ replaced by $\boldsymbol{H}'$ and $\boldsymbol{G}'$, respectively). Finally, the boundary of $\mathcal{C}_{\mathrm{R-E}}^{\mathrm{PS}}(P)$ can be obtained by taking a union operation over different $\mathcal{R}^{\mathrm{PS}}(P, \{\rho_i\})$'s with all possible ρ_i's.

In particular, we consider two special cases of the PS scheme: i) *Uniform Power Splitting* (UPS) with $\rho_i = \rho, \forall i$, and $0 \leq \rho \leq 1$; and ii) *On-Off Power Splitting* with $\rho_i \in \{0, 1\}, \forall i$, i.e., ρ_i taking the value of either 0 or 1. For the case of on-off power splitting, let $\Omega \subseteq \{1, \ldots, N\}$ denote one subset of receiving antennas with $\rho_i = 1$; then $\bar{\Omega} = \{1, \ldots, N\} - \Omega$ denotes the other subset of receiving antennas with $\rho_i = 0$. Clearly, Ω and $\bar{\Omega}$ specify the sets of receiving antennas switched to EH and ID receivers, respectively; thus, the on-off power splitting is also termed *Antenna Switching* (AS).

Let $\mathcal{R}^{\mathrm{UPS}}(P, \rho)$ denote the achievable R-E region for the UPS scheme with any fixed ρ, and $\mathcal{C}_{\mathrm{R-E}}^{\mathrm{UPS}}(P)$ be the R-E

region by taking the union of all $\mathcal{R}^{\mathrm{UPS}}(P, \rho)$'s over $0 \leq \rho \leq 1$. Furthermore, let $\mathcal{R}^{\mathrm{AS}}(P, \Omega)$ denote the achievable R-E region for the AS (or On-Off Power Splitting) scheme with a given pair of Ω and $\bar{\Omega}$. It is not difficult to see that for any $P > 0$, $\mathcal{C}_{\mathrm{R-E}}^{\mathrm{UPS}}(P) \subseteq \mathcal{C}_{\mathrm{R-E}}^{\mathrm{PS}}(P)$, and $\mathcal{R}^{\mathrm{AS}}(P, \Omega) \subseteq \mathcal{C}_{\mathrm{R-E}}^{\mathrm{PS}}(P), \forall \Omega$, while $\mathcal{C}_{\mathrm{R-E}}^{\mathrm{UPS}}(P) = \mathcal{C}_{\mathrm{R-E}}^{\mathrm{PS}}(P)$ for the case of MISO/SISO channel of $\boldsymbol{H}$. Moreover, the following proposition shows that for the case of SIMO channel of $\boldsymbol{H}$, $\mathcal{C}_{\mathrm{R-E}}^{\mathrm{UPS}}(P) = \mathcal{C}_{\mathrm{R-E}}^{\mathrm{PS}}(P)$ is also true.

Proposition 4.2: In the case of co-located EH and ID receivers with a SIMO channel $\boldsymbol{H} \equiv \boldsymbol{h} \in \mathbb{C}^{N \times 1}$, for any $P \geq 0$, $\mathcal{C}_{\mathrm{R-E}}^{\mathrm{UPS}}(P) = \mathcal{C}_{\mathrm{R-E}}^{\mathrm{PS}}(P) = \{(R, Q) : R \leq \log(1 + (\|\boldsymbol{h}\|^2 P - Q)), 0 \leq Q \leq \|\boldsymbol{h}\|^2 P\}$.

Proof: See Appendix F. ∎

D. Performance Comparison

The following proposition summarizes the performance comparison between the TS and UPS schemes.

Proposition 4.3: For the co-located EH and ID receivers, with any $P > 0$, $\mathcal{C}_{\mathrm{R-E}}^{\mathrm{TS}_1}(P) \subseteq \mathcal{C}_{\mathrm{R-E}}^{\mathrm{UPS}}(P) \subseteq \mathcal{C}_{\mathrm{R-E}}^{\mathrm{TS}_2}(P)$, while $\mathcal{C}_{\mathrm{R-E}}^{\mathrm{UPS}}(P) = \mathcal{C}_{\mathrm{R-E}}^{\mathrm{TS}_2}(P)$ iff $P \leq (1/h_2 - 1/h_1)$.

Proof: See Appendix G. ∎

From the above proposition, it follows that the TS scheme with the fixed power constraint performs worse than the UPS scheme in terms of achievable rate-energy pairs. However, the UPS scheme in general performs worse than the TS scheme under the flexible power constraint (without any peak power constraint), while they perform identically iff the condition $P \leq (1/h_2 - 1/h_1)$ is satisfied. This may occur when, e.g., P is sufficiently small (unlikely in our model since high SNR is of interest), or $h_2 = 0$ (i.e., $\boldsymbol{H}$ is MISO or SIMO). Note that the performance comparison between the TS scheme (with the flexible power constraint) and the PS scheme with arbitrary power splitting (instead of UPS) remains unknown theoretically.

Next, for the purpose of exposition, we compare the rate-energy tradeoff for the case of co-located EH and ID receivers for a symmetric MIMO channel $\boldsymbol{G} = \boldsymbol{H} = [1, \; \theta; \theta, \; 1]$ with $\theta = 0.5$ for Fig. 7 and $\theta = 0.8$ for Fig. 8, respectively. It is assumed that $P = 100$. The R-E region outer bound is obtained as $\mathcal{C}_{\mathrm{R-E}}(P)$ with $\boldsymbol{G} = \boldsymbol{H}$ according to Corollary 4.1. The two achievable R-E regions for the TS scheme with fixed vs. flexible power constraints are shown for comparison, and it is observed that $\mathcal{C}_{\mathrm{R-E}}^{\mathrm{TS}_1}(P) \subseteq \mathcal{C}_{\mathrm{R-E}}^{\mathrm{TS}_2}(P)$. The achievable R-E region for the TS scheme with the flexible power constraint P as well as the peak power constraint $P_{\mathrm{peak}} = 2P$ is also shown, which is observed to lie between $\mathcal{C}_{\mathrm{R-E}}^{\mathrm{TS}_1}(P)$ and $\mathcal{C}_{\mathrm{R-E}}^{\mathrm{TS}_2}(P)$. Moreover, the achievable R-E region $\mathcal{C}_{\mathrm{R-E}}^{\mathrm{UPS}}(P)$ for the UPS scheme is shown, whose boundary points constitute those of $\mathcal{R}^{\mathrm{UPS}}(P, \rho)$'s with different ρ's from 0 to 1. It is observed that $\mathcal{C}_{\mathrm{R-E}}^{\mathrm{TS}_1}(P) \subseteq \mathcal{C}_{\mathrm{R-E}}^{\mathrm{UPS}}(P) \subseteq \mathcal{C}_{\mathrm{R-E}}^{\mathrm{TS}_2}(P)$, which is in accordance with Proposition 4.3. Note that for this channel, the R-E region $\mathcal{C}_{\mathrm{R-E}}^{\mathrm{PS}}(P)$ for the general PS scheme defined in (13) only provides negligible rate-energy gains over $\mathcal{C}_{\mathrm{R-E}}^{\mathrm{UPS}}(P)$ by the UPS scheme, and is thus not shown here. In addition, the achievable R-E
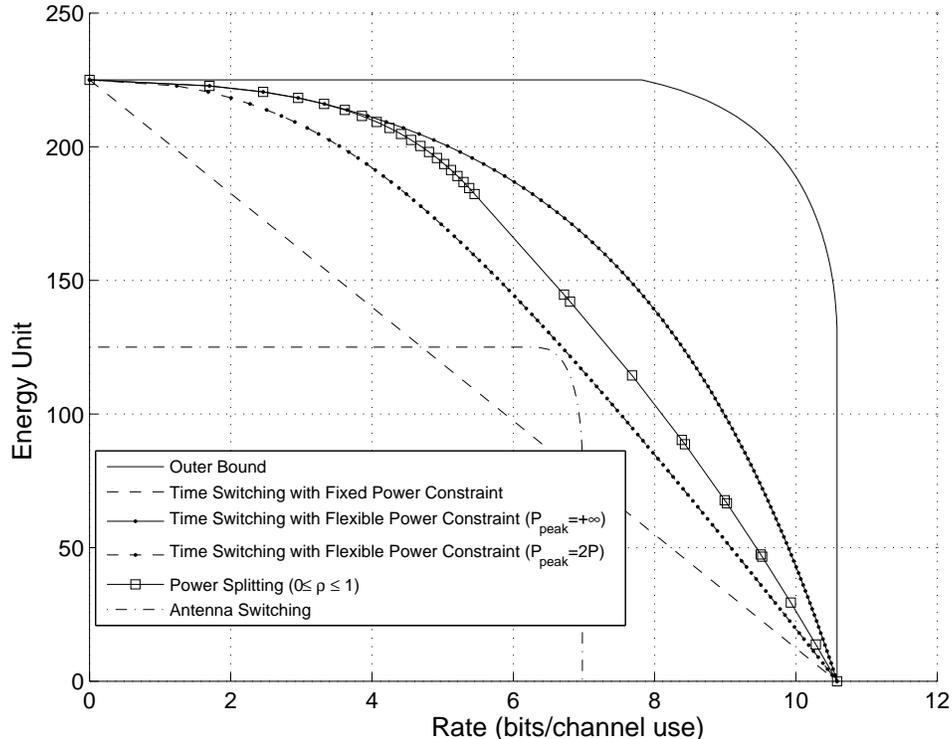
Fig. 7. Rate-energy tradeoff for a 2×2 MIMO broadcast system with co-located EH and ID receivers, and $\boldsymbol{H} = [1\ 0.5; 0.5\ 1]$.

region $\mathcal{R}^{\mathrm{AS}}(P, \Omega)$ for the AS scheme is shown, which is the same for $\Omega = \{1\}$ or $\{2\}$ due to the symmetric channel setup. Furthermore, by comparing Figs. 7 and 8, it is observed that the performance gap between $\mathcal{C}_{\mathrm{R-E}}^{\mathrm{UPS}}(P)$ and $\mathcal{C}_{\mathrm{R-E}}^{\mathrm{TS_2}}(P)$ is reduced when θ increases from 0.5 to 0.8. This is because for this channel setup, $h_1 = (1 + \theta)^2$ and $h_2 = (1 - \theta)^2$, and as a result, the condition $P \leq (1/h_2 - 1/h_1)$ in Proposition 4.3 for $\mathcal{C}_{\mathrm{R-E}}^{\mathrm{UPS}}(P) = \mathcal{C}_{\mathrm{R-E}}^{\mathrm{TS_2}}(P)$ will hold when $\theta \to 1$ for any $P > 0$. Finally, it is worth pointing out that in practical SWIPT systems with the co-located EH/ID receiver, under the high-SNR condition, the receiver typically operates at the "high-energy" regime in the achievable rate-energy regions shown in Figs. 7 and 8, which corresponds to applying very large values of the time-switching coefficient α or the power-splitting coefficient ρ, i.e, $\alpha \to 1$ and $\rho \to 1$.

V. CONCLUDING REMARKS

This paper investigated the performance limits of emerging "wireless-powered" communication networks by means of opportunistic energy harvesting from ambient radio signals or dedicated wireless power transfer. Under a simplified three-node setup, our study revealed some fundamental tradeoffs in designing wireless MIMO systems for maximizing the efficiency of simultaneous information and energy transmission. Due to the space limitation, there are serval important issues unaddressed in this paper and left for our future work, some of which are highlighted as follows:

- It will be interesting to extend the rate-energy region characterization to more general MIMO broadcast systems
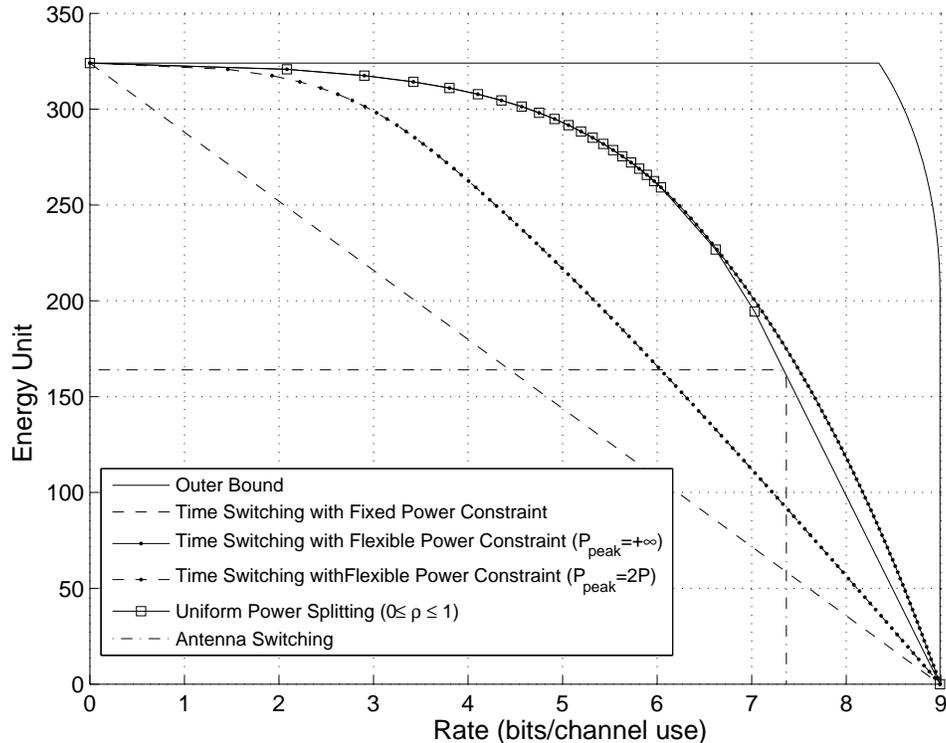
Fig. 8. Rate-energy tradeoff for a 2×2 MIMO broadcast system with co-located EH and ID receivers, and $\boldsymbol{H} = [1\ 0.8; 0.8\ 1]$.

with more than two receivers. Depending on whether the energy and information receivers are separated or co-located, and the broadcast information is for unicasting or multicasting, various new problems can be formulated for which the optimal solutions are challenging to obtain.

- For the case of co-located energy and information receivers, this paper shows a performance bound that in general cannot be achieved by practical receivers. Although this paper has shed some light on practical hardware designs to approach this limit (e.g., by the power splitting scheme), further research endeavor is still required to further reduce or close this gap, even for the SISO AWGN channel.

- In this paper, to simplify the analysis, it is assumed that the energy conversion efficiency at the energy receiver is independent of the instantaneous amplitude of the received radio signal, which is in general not true for practical RF energy harvesting circuits [21]. Thus, how to design the broadcast signal waveform, namely *energy modulation*, to maximize the efficiency of energy transfer to multiple receivers under practical energy conversion constraints is an open problem of high practical interests.

- Unlike the traditional view that the receiver noise and/or co-channel interference degrade the communication link reliability [22], they are however beneficial from the viewpoint of RF energy harvesting. Thus, there exist nontrivial tradeoffs in allocating communication resources to optimize the network interference levels for achieving maximal information vs. energy transfer. More studies to reveal such tradeoffs are worth pursuing.

APPENDIX A

PROOF OF PROPOSITION 2.1

Without loss of generality, we can write the optimal solution to Problem (P1) in its eigenvalue decomposition form as $\boldsymbol{S}_{\text{EH}} = \boldsymbol{V}\boldsymbol{\Sigma}\boldsymbol{V}^H$, where $\boldsymbol{V} \in \mathbb{C}^{M \times M}$, $\boldsymbol{V}\boldsymbol{V}^H = \boldsymbol{V}^H\boldsymbol{V} = \boldsymbol{I}$, and $\boldsymbol{\Sigma} = \texttt{diag}(p_1, \ldots, p_M)$ with $p_1 \geq p_2 \geq \ldots \geq p_M \geq 0$ and $\sum_{i=1}^{M} p_i \leq P$. Let $\hat{\boldsymbol{G}} = \boldsymbol{G}\boldsymbol{V} = [\hat{\boldsymbol{g}}_1, \ldots, \hat{\boldsymbol{g}}_M]$. Then, the objective function of Problem (P1) can be written as $Q = \texttt{tr}(\boldsymbol{G}\boldsymbol{S}\boldsymbol{G}^H) = \texttt{tr}(\hat{\boldsymbol{G}}\boldsymbol{\Sigma}\hat{\boldsymbol{G}}^H) = \sum_{i=1}^{M} p_i\|\hat{\boldsymbol{g}}_i\|^2 \leq P\|\hat{\boldsymbol{g}}_1\|^2$, where the equality holds if $\|\hat{\boldsymbol{g}}_1\|^2 = \max_i \|\hat{\boldsymbol{g}}_i\|^2$ and $p_1 = P, p_i = 0, i = 2, \ldots, M$. Let $\boldsymbol{V} = [\boldsymbol{v}_1, \ldots, \boldsymbol{v}_M]$. Since the (reduced) SVD of $\boldsymbol{G}$ is given by $\boldsymbol{G} = \boldsymbol{U}_G\boldsymbol{\Gamma}_G^{1/2}\boldsymbol{V}_G^H$ in Section II, we infer that $\|\hat{\boldsymbol{g}}_1\|^2$ is the maximum of all $\|\hat{\boldsymbol{g}}_i\|^2$'s if and only if $\boldsymbol{v}_1$ is the first column of $\boldsymbol{V}_G$ corresponding to the largest singular value of $\boldsymbol{G}$, which is $\sqrt{g_1}$. Hence, we obtain the optimal solution of Problem (P1) as $\boldsymbol{S}_{\text{EH}} = P\boldsymbol{v}_1\boldsymbol{v}_1^H$. The proof of Proposition 2.1 is thus completed.

APPENDIX B

PROOF OF THEOREM 3.1

The Lagrangian of (P3) can be written as

$$L(\boldsymbol{S}, \lambda, \mu) = \log\left|\boldsymbol{I} + \boldsymbol{H}\boldsymbol{S}\boldsymbol{H}^H\right| + \lambda\left(\texttt{tr}\left(\boldsymbol{G}\boldsymbol{S}\boldsymbol{G}^H\right) - \bar{Q}\right) - \mu\left(\texttt{tr}(\boldsymbol{S}) - P\right). \tag{14}$$

Then, the Lagrange dual function of (P3) is defined as $g(\lambda, \mu) = \max_{\boldsymbol{S} \succeq 0} L(\boldsymbol{S}, \lambda, \mu)$, and the dual problem of (P3), denoted as (P3-D), is defined as $\min_{\lambda \geq 0, \mu \geq 0} g(\lambda, \mu)$. Since (P3) can be solved equivalently by solving (P3-D), in the following, we first maximize the Lagrangian to obtain the dual function with fixed $\lambda \geq 0$ and $\mu \geq 0$, and then find the optimal dual solutions λ^* and μ^* to minimize the dual function. The transmit covariance $\boldsymbol{S}^*$ that maximizes the Lagrangian to obtain $g(\lambda^*, \mu^*)$ is thus the optimal primal solution of (P3).

Consider first the problem of maximizing the Lagrangian over $\boldsymbol{S}$ with fixed λ and μ. By discarding the constant terms associated with λ and μ in (14), this problem can be equivalently rewritten as

$$\max_{\boldsymbol{S} \succeq 0} \log\left|\boldsymbol{I} + \boldsymbol{H}\boldsymbol{S}\boldsymbol{H}^H\right| - \texttt{tr}\left(\left(\mu\boldsymbol{I} - \lambda\boldsymbol{G}^H\boldsymbol{G}\right)\boldsymbol{S}\right). \tag{15}$$

Recall that g_1 is the largest eigenvalue of the matrix $\boldsymbol{G}^H\boldsymbol{G}$. We then have the following lemma.

<u>*Lemma B.1:*</u> For the problem in (15) to have a bounded optimal value, $\mu > \lambda g_1$ must hold.

Proof: We prove this lemma by contradiction. Suppose that $\mu \leq \lambda g_1$. Then, let $\boldsymbol{S}^\star = \beta\boldsymbol{v}_1\boldsymbol{v}_1^H$ with β being any positive constant. Substituting $\boldsymbol{S}^\star$ into (15) yields $\log(1 + \beta\|\boldsymbol{H}\boldsymbol{v}_1\|^2) + \beta(\lambda g_1 - \mu)$. Since $\boldsymbol{H}$ and $\boldsymbol{G}$ are either independent (in the case of separated receivers) or identical (in the case of co-located receivers), it is valid to assume that $\|\boldsymbol{H}\boldsymbol{v}_1\|^2 > 0$ and thus the value of the above function or the optimal value of Problem (15) becomes unbounded when $\beta \to \infty$. Thus, the presumption that $\mu \leq \lambda g_1$ cannot be true, which completes the proof. ∎

TABLE I

ALGORITHM FOR SOLVING PROBLEM (P3).

Initialize $\lambda \geq 0, \mu \geq 0, \mu > \lambda g_1$
Repeat
Compute $\boldsymbol{S}^\star$ using (17) with the given λ and μ
Compute the subgradient of $g(\lambda, \mu)$
Update λ and μ using the ellipsoid method subject to $\mu > \lambda g_1 \geq 0$
Until λ and μ converge to the prescribed accuracy
Set $\boldsymbol{S}^* = \boldsymbol{S}^\star$

Since Problem (P3) should have a bounded optimal value, it follows from the above lemma that the optimal primal and dual solutions of (P3) are obtained when $\mu > \lambda g_1$. Let $\boldsymbol{A} = \mu \boldsymbol{I} - \lambda \boldsymbol{G}^H \boldsymbol{G}$. It then follows that $\boldsymbol{A} \succ 0$ with $\mu > \lambda g_1$, and thus $\boldsymbol{A}^{-1}$ exists. The problem in (15) is then rewritten as

$$\max_{\boldsymbol{S} \succeq 0} \log \left| \boldsymbol{I} + \boldsymbol{H} \boldsymbol{S} \boldsymbol{H}^H \right| - \mathrm{tr}\left(\boldsymbol{A} \boldsymbol{S} \right). \tag{16}$$

Let the (reduced) SVD of the matrix $\boldsymbol{H} \boldsymbol{A}^{-1/2}$ be given by $\boldsymbol{H} \boldsymbol{A}^{-1/2} = \tilde{\boldsymbol{U}} \tilde{\boldsymbol{\Gamma}}^{1/2} \tilde{\boldsymbol{V}}^H$, where $\tilde{\boldsymbol{U}} \in \mathbb{C}^{M \times T_2}$, $\tilde{\boldsymbol{V}} \in \mathbb{C}^{M \times T_2}$, $\tilde{\boldsymbol{\Gamma}} = \mathrm{diag}(\tilde{h}_1, \ldots, \tilde{h}_{T_2})$, with $\tilde{h}_1 \geq \tilde{h}_2 \geq \ldots \geq \tilde{h}_{T_2} \geq 0$. It has been shown in [17] under the CR setup that the optimal solution to Problem (16) with arbitrary $\boldsymbol{A} \succ 0$ has the following form:

$$\boldsymbol{S}^\star = \boldsymbol{A}^{-1/2} \tilde{\boldsymbol{V}} \tilde{\boldsymbol{\Lambda}} \tilde{\boldsymbol{V}}^H \boldsymbol{A}^{-1/2} \tag{17}$$

where $\tilde{\boldsymbol{\Lambda}} = \mathrm{diag}(\tilde{p}_1, \ldots, \tilde{p}_{T_2})$, with $\tilde{p}_i = (1 - 1/\tilde{h}_i)^+, i = 1, \ldots, T_2$.

Next, we address how to solve the dual problem (P3-D) by minimizing the dual function $g(\lambda, \mu)$ subject to $\lambda \geq 0$, $\mu \geq 0$, and the new constraint $\mu > \lambda g_1$. This can be done by applying the subgradient-based method, e.g., the ellipsoid method [20], for which it can be shown (the proof is omitted for brevity) that the subgradient of $g(\lambda, \mu)$ at point $[\lambda, \mu]$ is given by $[\mathrm{tr}(\boldsymbol{G} \boldsymbol{S}^\star \boldsymbol{G}^H) - \bar{Q}, P - \mathrm{tr}(\boldsymbol{S}^\star)]$, where $\boldsymbol{S}^\star$ is given in (17), which is the optimal solution of Problem (15) for a given pair of λ and μ. When the optimal dual solutions λ^* and μ^* are obtained by the ellipsoid method, the corresponding optimal solution $\boldsymbol{S}^\star$ for Problem (15) converges to the primal optimal solution to Problem (P3), denoted by $\boldsymbol{S}^*$. The above procedures for solving (P3) are summarized in Table I. The proof of Theorem 3.1 is thus completed.

APPENDIX C

PROOF OF COROLLARY 3.1

Since $\boldsymbol{H} \equiv \boldsymbol{h}^H$, in Theorem 3.1, the (reduced) SVD of $\boldsymbol{h}^H \boldsymbol{A}^{-1/2}$ with $\boldsymbol{A} = \mu^* \boldsymbol{I} - \lambda^* \boldsymbol{G}^H \boldsymbol{G}$ simplifies to $\boldsymbol{h}^H \boldsymbol{A}^{-1/2} = 1 \times \sqrt{\tilde{h}_1} \times \tilde{\boldsymbol{v}}_1^H$, where $\tilde{h}_1 = \|\boldsymbol{A}^{-1/2} \boldsymbol{h}\|^2$ and $\tilde{\boldsymbol{v}}_1 = \boldsymbol{A}^{-1/2} \boldsymbol{h} / \|\boldsymbol{A}^{-1/2} \boldsymbol{h}\|$. Thus, from (5) we have

$$\boldsymbol{S}^* = \boldsymbol{A}^{-1/2}\tilde{\boldsymbol{v}}_1\tilde{p}_1\tilde{\boldsymbol{v}}_1^H\boldsymbol{A}^{-1/2} \tag{18}$$

$$= \frac{\boldsymbol{A}^{-1/2}\boldsymbol{A}^{-1/2}\boldsymbol{h}}{\|\boldsymbol{A}^{-1/2}\boldsymbol{h}\|}\left(1 - \frac{1}{\|\boldsymbol{A}^{-1/2}\boldsymbol{h}\|^2}\right)^+ \frac{\boldsymbol{h}^H\boldsymbol{A}^{-1/2}\boldsymbol{A}^{-1/2}}{\|\boldsymbol{A}^{-1/2}\boldsymbol{h}\|} \tag{19}$$

$$= \boldsymbol{A}^{-1}\boldsymbol{h}\left(\frac{1}{\|\boldsymbol{A}^{-1/2}\boldsymbol{h}\|^2} - \frac{1}{\|\boldsymbol{A}^{-1/2}\boldsymbol{h}\|^4}\right)^+ \boldsymbol{h}^H\boldsymbol{A}^{-1}. \tag{20}$$

Moreover, since $T_2 = 1$ in this case, the maximum achievable rate is given by

$$R^* = \sum_{i=1}^{T_2}\log(1 + \tilde{h}_i\tilde{p}_i) = \sum_{i=1}^{T_2}\left(\log(\tilde{h}_i)\right)^+ = \left(2\log\left(\|\boldsymbol{A}^{-1/2}\boldsymbol{h}\|\right)\right)^+. \tag{21}$$

From (20) and (21), Corollary 3.1 thus follows.

APPENDIX D
PROOF OF COROLLARY 4.1

Since $\boldsymbol{G} = \boldsymbol{H}$, from Theorem 3.1, we have $\boldsymbol{A} = \mu^*\boldsymbol{I} - \lambda^*\boldsymbol{G}^H\boldsymbol{G} = \mu^*\boldsymbol{I} - \lambda^*\boldsymbol{H}^H\boldsymbol{H} \succ 0$ (i.e., $\mu^* > \lambda^* h_1$).

Recall that the (reduced) SVD of $\boldsymbol{H}$ is given by $\boldsymbol{H} = \boldsymbol{U}_H\boldsymbol{\Gamma}_H^{1/2}\boldsymbol{V}_H^H$, with $\boldsymbol{\Gamma}_H = \mathtt{diag}(h_1, \ldots, h_{T_2})$, $h_1 \geq h_2 \geq$

$\ldots \geq h_{T_2} \geq 0$. Thus, it follows that $\boldsymbol{A} = \mu^*\boldsymbol{I} - \lambda^*\boldsymbol{H}^H\boldsymbol{H} = \boldsymbol{V}_H(\mu^*\boldsymbol{I} - \lambda^*\boldsymbol{\Gamma}_H)\boldsymbol{V}_H^H$, and $\boldsymbol{A}^{-1/2} = \boldsymbol{V}_H(\mu^*\boldsymbol{I} -$

$\lambda^*\boldsymbol{\Gamma}_H)^{-1/2}\boldsymbol{V}_H^H$. Then, the (reduced) SVD of the matrix $\boldsymbol{H}\boldsymbol{A}^{-1/2}$ is given by $\boldsymbol{H}(\boldsymbol{V}_H(\mu^*\boldsymbol{I} - \lambda^*\boldsymbol{\Gamma}_H)\boldsymbol{V}_H^H)^{-1/2} =$

$\boldsymbol{U}_H\boldsymbol{\Gamma}_H^{1/2}(\mu^*\boldsymbol{I} - \lambda^*\boldsymbol{\Gamma}_H)^{-1/2}\boldsymbol{V}_H^H$. Since in Theorem 3.1, the SVD of $\boldsymbol{H}\boldsymbol{A}^{-1/2}$ is denoted by $\tilde{\boldsymbol{U}}\tilde{\boldsymbol{\Gamma}}^{1/2}\tilde{\boldsymbol{V}}^H$, we thus

obtain $\tilde{\boldsymbol{U}} = \boldsymbol{U}_H$, $\tilde{\boldsymbol{\Gamma}} = \boldsymbol{\Gamma}_H(\mu^*\boldsymbol{I} - \lambda^*\boldsymbol{\Gamma}_H)^{-1}$, and $\tilde{\boldsymbol{V}} = \boldsymbol{V}_H$. From (5), it then follows that

$$\boldsymbol{S}^* = \boldsymbol{A}^{-1/2}\tilde{\boldsymbol{V}}\tilde{\boldsymbol{\Lambda}}\tilde{\boldsymbol{V}}^H\boldsymbol{A}^{-1/2} \tag{22}$$

$$= \boldsymbol{V}_H(\mu^*\boldsymbol{I} - \lambda^*\boldsymbol{\Gamma}_H)^{-1/2}\boldsymbol{V}_H^H\boldsymbol{V}_H\tilde{\boldsymbol{\Lambda}}\boldsymbol{V}_H^H\boldsymbol{V}_H(\mu^*\boldsymbol{I} - \lambda^*\boldsymbol{\Gamma}_H)^{-1/2}\boldsymbol{V}_H \tag{23}$$

$$= \boldsymbol{V}_H(\mu^*\boldsymbol{I} - \lambda^*\boldsymbol{\Gamma}_H)^{-1}\tilde{\boldsymbol{\Lambda}}\boldsymbol{V}_H^H \tag{24}$$

$$\triangleq \boldsymbol{V}_H\boldsymbol{\Sigma}\boldsymbol{V}_H^H \tag{25}$$

where $\boldsymbol{\Sigma} = (\mu^*\boldsymbol{I} - \lambda^*\boldsymbol{\Gamma}_H)^{-1}\tilde{\boldsymbol{\Lambda}} \triangleq \mathtt{diag}(\hat{p}_1, \ldots, \hat{p}_{T_2})$. Note that in Theorem 3.1, $\tilde{\boldsymbol{\Lambda}} = \mathtt{diag}(\tilde{p}_1, \ldots, \tilde{p}_{T_2})$, with

$\tilde{p}_i = (1 - 1/\tilde{h}_i)^+, i = 1, \ldots, T_2$, and $\tilde{\boldsymbol{\Gamma}} = \mathtt{diag}(\tilde{h}_1, \ldots, \tilde{h}_{T_2}) = \boldsymbol{\Gamma}_H(\mu^*\boldsymbol{I} - \lambda^*\boldsymbol{\Gamma}_H)^{-1}$. Thus, we obtain that

$$\hat{p}_i = \frac{1}{\mu^* - \lambda^* h_i}\left(1 - \frac{\mu^* - \lambda^* h_i}{h_i}\right)^+ \tag{26}$$

$$= \left(\frac{1}{\mu^* - \lambda^* h_i} - \frac{1}{h_i}\right)^+, \quad i = 1, \ldots, T_2. \tag{27}$$

Moreover, it is easy to verify that $\boldsymbol{\Gamma}_H\boldsymbol{\Sigma} = \tilde{\boldsymbol{\Gamma}}\tilde{\boldsymbol{\Lambda}}$. Since for Problem (P3), the maximum achievable rate is given by

$R^* = \sum_{i=1}^{T_2}\log(1 + \tilde{h}_i\tilde{p}_i)$, it follows that

$$R^* = \sum_{i=1}^{T_2}\log(1 + h_i\hat{p}_i). \tag{28}$$

With (25), (27), and (28), the proof of Corollary 4.1 is thus completed.

APPENDIX E

PROOF OF PROPOSITION 4.1

Due to orthogonal transmissions for the EH and ID receivers in the TS scheme, we first show that the minimum transmission energy consumed to achieve any harvested power $Q < Q_{\max}$ in the EH time slot is equal to Q/h_1 regardless of α, as follows: From Section II (assuming $\boldsymbol{G} = \boldsymbol{H}$), it follows that the optimal $\boldsymbol{S}_2$ is in the form of $q\boldsymbol{v}_1\boldsymbol{v}_1^H$, where $q > 0$ and $\boldsymbol{v}_1$ is the eigenvector of the matrix $\boldsymbol{H}^H\boldsymbol{H}$ corresponding to its largest eigenvalue denoted by h_1. To achieve Q, it follows from (11) that $\alpha\mathtt{tr}(\boldsymbol{H}\boldsymbol{S}_2\boldsymbol{H}^H) = Q$ and thus $q = Q/(h_1\alpha)$. Thus, the minimum energy consumed to achieve Q in (11) is given by $\alpha\mathtt{tr}(\boldsymbol{S}_2) = \alpha \cdot q = Q/h_1$, independent of α.

With this result, in (11), the transmission rate R is given by $(1-\alpha)\log|\boldsymbol{I}+\boldsymbol{H}\boldsymbol{S}_1\boldsymbol{H}^H|$ subject to $(1-\alpha)\mathtt{tr}(\boldsymbol{S}_1) \leq (P - Q/h_1)$. Due to the concavity of the $\log(\cdot)$ function, it follows that R is maximized when $\alpha \to 0$, under which the optimal solution of $\boldsymbol{S}_1$ can be obtained similarly as for Problem (P2). Thus, by changing the values of Q in the interval of $0 < Q < Q_{\max}$ and solving the above problem with $\alpha = 0$, the corresponding maximum achievable rates as well as the boundary of $\mathcal{C}_{\mathrm{R-E}}^{\mathrm{TS}_2}(P)$ are obtained as given in (12) for the case of flexible power constraint. Proposition 4.1 thus follows.

APPENDIX F

PROOF OF PROPOSITION 4.2

Since $\boldsymbol{H} \equiv \boldsymbol{h} \triangleq [h_1,\ldots,h_N]^T$, for any set of ρ_i's with $0 \leq \rho_i \leq 1$, the harvested power is equal to $Q = P\sum_{i=1}^N \rho_i|h_i|^2$. Clearly, $0 \leq Q \leq \|\boldsymbol{h}\|^2 P$. The equivalent SIMO channel for decoding information then becomes $\tilde{\boldsymbol{h}} \triangleq [\sqrt{1-\rho_1}h_1,\ldots,\sqrt{1-\rho_N}h_N]^T$. Since for the SIMO channel, the transmit covariance matrix degrades to a scalar equal to P, the maximum achievable rate is given by (via applying the MRC beamforming at ID receiver):

$$R = \log\left(1 + \|\tilde{\boldsymbol{h}}\|^2 P\right) \tag{29}$$

$$= \log\left(1 + \sum_{i=1}^N (1-\rho_i)|h_i|^2 P\right) \tag{30}$$

$$= \log\left(1 + \sum_{i=1}^N |h_i|^2 P - \sum_{i=1}^N \rho_i|h_i|^2 P\right) \tag{31}$$

$$= \log\left(1 + \|\boldsymbol{h}\|^2 P - Q\right). \tag{32}$$

We thus have $\mathcal{C}_{\mathrm{R-E}}^{\mathrm{PS}}(P) = \{(R,Q) : R \leq \log(1 + (\|\boldsymbol{h}\|^2 P - Q)), 0 \leq Q \leq \|\boldsymbol{h}\|^2 P\}$. Furthermore, since the above proof is valid for any ρ_i's and changing ρ from 0 to 1 yields the value of $Q = P\rho\sum_{i=1}^N |h_i|^2$ from 0 to $\|\boldsymbol{h}\|^2 P$, it thus follows that $\mathcal{C}_{\mathrm{R-E}}^{\mathrm{UPS}}(P) = \{(R,Q) : R \leq \log(1 + (\|\boldsymbol{h}\|^2 P - Q)), 0 \leq Q \leq \|\boldsymbol{h}\|^2 P\}$, which is the same as $\mathcal{C}_{\mathrm{R-E}}^{\mathrm{PS}}(P)$. The proof of Proposition 4.2 is thus completed.

APPENDIX G

PROOF OF PROPOSITION 4.3

First, we prove the former part of Proposition 4.3, i.e., for any $P > 0$, $\mathcal{C}_{\text{R-E}}^{\text{TS}_1}(P) \subseteq \mathcal{C}_{\text{R-E}}^{\text{UPS}}(P) \subseteq \mathcal{C}_{\text{R-E}}^{\text{TS}_2}(P)$. The proof of $\mathcal{C}_{\text{R-E}}^{\text{TS}_1}(P) \subseteq \mathcal{C}_{\text{R-E}}^{\text{UPS}}(P)$ is trivial, since the boundary of $\mathcal{C}_{\text{R-E}}^{\text{TS}_1}(P)$ is simply a straight line connecting the two boundary points $(0, Q_{\max})$ and $(R_{\max}, 0)$ (cf. Fig. 7), and $\mathcal{C}_{\text{R-E}}^{\text{UPS}}(P)$ is a convex set containing these two points. Next, we prove $\mathcal{C}_{\text{R-E}}^{\text{UPS}}(P) \subseteq \mathcal{C}_{\text{R-E}}^{\text{TS}_2}(P), \forall P \geq 0$, by showing that for any given harvested power $0 < Q < Q_{\max}$, the corresponding boundary rate for $\mathcal{C}_{\text{R-E}}^{\text{TS}_2}(P)$, denoted by R_{TS}, is no smaller than that for $\mathcal{C}_{\text{R-E}}^{\text{UPS}}(P)$, denoted by R_{UPS}, i.e., $R_{\text{TS}} \geq R_{\text{UPS}}$, as follows: For any given Q, from the proof of Proposition 4.1, it follows that R_{TS} is obtained (with $\alpha = 0$) by maximizing $\log|\boldsymbol{I} + \boldsymbol{H}\boldsymbol{S}_1\boldsymbol{H}^H|$ subject to $\texttt{tr}(\boldsymbol{S}_1) \leq (P - Q/h_1)$. On the other hand, for the UPS scheme, from the harvested power constraint $\rho\,\texttt{tr}\left(\boldsymbol{H}\boldsymbol{S}\boldsymbol{H}^H\right) \geq Q$, it follows that $\rho \geq Q/(h_1P)$ must hold. Note that R_{UPS} is obtained by maximizing $\log\left|\boldsymbol{I} + (1-\rho)\boldsymbol{H}\boldsymbol{S}\boldsymbol{H}^H\right|$ subject to $\texttt{tr}(\boldsymbol{S}) \leq P$. Let $\boldsymbol{S}' = (1-\rho)\boldsymbol{S}$. The above problem then becomes equivalent to maximizing $\log\left|\boldsymbol{I} + \boldsymbol{H}\boldsymbol{S}'\boldsymbol{H}^H\right|$ subject to $\texttt{tr}(\boldsymbol{S}') \leq (1-\rho)P$. Since $\rho \geq Q/(h_1P)$, it follows that $\texttt{tr}(\boldsymbol{S}') \leq (1 - Q/(h_1P))P = P - Q/h_1$. Thus, it follows that $R_{\text{TS}} \geq R_{\text{UPS}}$. The former part of Proposition 4.3 is proved.

Next, we show the latter part of Proposition 4.3, i.e., $\mathcal{C}_{\text{R-E}}^{\text{UPS}}(P) = \mathcal{C}_{\text{R-E}}^{\text{TS}_2}(P)$ iff $P \leq (1/h_2 - 1/h_1)$. Consider first the proof of the "if" part. For any $0 < Q < Q_{\max}$, since $R_{\text{TS}} = \max_{\boldsymbol{S}_1} \log|\boldsymbol{I} + \boldsymbol{H}\boldsymbol{S}_1\boldsymbol{H}^H|$ subject to $\texttt{tr}(\boldsymbol{S}_1) \leq (P - Q/h_1) < (1/h_2 - 1/h_1)$, the optimal solution for this problem must be beamforming, i.e., $\boldsymbol{S}_1 = (P - Q/h_1)\boldsymbol{v}_1\boldsymbol{v}_1^H$ with $\boldsymbol{v}_1$ being the eigenvector of $\boldsymbol{H}^H\boldsymbol{H}$ corresponding to its largest eigenvalue h_1, due to the WF power application given by (3). Thus, it follows that $R_{\text{TS}} = \log(1 + h_1P - Q)$. Consider now the UPS scheme. Suppose that $\boldsymbol{S} = P\boldsymbol{v}_1\boldsymbol{v}_1^H$ and $\rho = Q/(h_1P)$. It then follows that for UPS, the harvested power is equal to $\rho\,\texttt{tr}\left(\boldsymbol{H}\boldsymbol{S}\boldsymbol{H}^H\right) = Q/(h_1P) \times (h_1P) = Q$, and the achievable rate R_{UPS} is equal to $\log\left|\boldsymbol{I} + (1-\rho)\boldsymbol{H}\boldsymbol{S}\boldsymbol{H}^H\right| = \log(1 + (1 - Q/(h_1P)) \times h_1P) = \log(1 + h_1P - Q) = R_{\text{TS}}$. Thus, we prove that $\mathcal{C}_{\text{R-E}}^{\text{UPS}}(P) \supseteq \mathcal{C}_{\text{R-E}}^{\text{TS}_2}(P)$. Since from the proof of the former part of Proposition 4.3 we have that $\mathcal{C}_{\text{R-E}}^{\text{UPS}}(P) \subseteq \mathcal{C}_{\text{R-E}}^{\text{TS}_2}(P)$, it thus follows that $\mathcal{C}_{\text{R-E}}^{\text{UPS}}(P) = \mathcal{C}_{\text{R-E}}^{\text{TS}_2}(P)$. The "if" part is proved.

Second, we prove the "only if" part by contradiction. Suppose that $\mathcal{C}_{\text{R-E}}^{\text{UPS}}(P) = \mathcal{C}_{\text{R-E}}^{\text{TS}_2}(P)$ for $P = 1/h_2 - 1/h_1 + \delta$ with arbitrary $\delta > 0$ and thus $P > (1/h_2 - 1/h_1)$. For any $0 < Q < h_1\delta$, the corresponding R_{TS} on the boundary of $\mathcal{C}_{\text{R-E}}^{\text{TS}_2}(P)$ is given by $\max_{\boldsymbol{S}_1} \log|\boldsymbol{I} + \boldsymbol{H}\boldsymbol{S}_1\boldsymbol{H}^H|$, where $\texttt{tr}(\boldsymbol{S}_1) = P - Q/h_1 > P - \delta = 1/h_2 - 1/h_1$. Since $\texttt{tr}(\boldsymbol{S}_1) > 1/h_2 - 1/h_1$, from the WF power allocation in (3) it follows that the optimal rank of $\boldsymbol{S}_1$ must be greater than one. Consider now the UPS scheme. Since $\mathcal{C}_{\text{R-E}}^{\text{UPS}}(P) = \mathcal{C}_{\text{R-E}}^{\text{TS}_2}(P)$, it follows that for the same Q as in the TS scheme, the maximum rate for the UPS scheme is $R_{\text{UPS}} = R_{\text{TS}}$. From the proof of the former part of Proposition 4.3, we know that to achieve Q with UPS, $\rho \geq Q/(h_1P)$ with the equality only when the transmit covariance is

rank-one. Furthermore, since R_{UPS} is equal to $\log\left|\boldsymbol{I} + \boldsymbol{H}\boldsymbol{S}'\boldsymbol{H}^H\right|$ with $\texttt{tr}(\boldsymbol{S}') = (1-\rho)P \leq P - Q/h_1$, where the equality holds only if $\boldsymbol{S}'$ is rank-one. Since $R_{\text{UPS}} = R_{\text{TS}}$, it thus follows that $\boldsymbol{S}' = \boldsymbol{S}_1$ and $\texttt{tr}(\boldsymbol{S}') = P - Q/h_1$ must hold at the same time. Since these two equalities require that $\boldsymbol{S}'$ have the rank greater than one and equal to one, respectively, they cannot hold at the same time. Thus, $R_{\text{UPS}} = R_{\text{TS}}$ cannot be true and the presumption that $\mathcal{C}_{\text{R-E}}^{\text{UPS}}(P) = \mathcal{C}_{\text{R-E}}^{\text{TS}_2}(P)$ does not hold. The "only if" part is proved.

Combining the proofs for both the "if" and "only if" parts, the latter part of Proposition 4.3 is thus proved.

References

[1] L. R. Varshney, "Transporting information and energy simultaneously," in *Proc. IEEE Int. Symp. Inf. Theory (ISIT)*, pp. 1612-1616, July 2008.

[2] P. Grover and A. Sahai, "Shannon meets Tesla: wireless information and power transfer," in *Proc. IEEE Int. Symp. Inf. Theory (ISIT)*, pp. 2363-2367, June 2010.

[3] R. Want, "Enabling ubiquitous sensing with RFID," *IEEE Computer*, vol. 37, pp. 84-86, Apr. 2004.

[4] G. Landis, M. Stavnes, S. Oleson, and J. Bozek, "Space transfer with ground-based laser/electric propulsion," *NASA Technical Memorandum*, TM-106060, 1992.

[5] F. Zhang *et al.*, "Wireless energy transfer platform for medical sensors and implantable devices," in *Proc. IEEE EMBS 31st Annual Int. Conf.*, pp. 1045-1048, Sep. 2009.

[6] I. E. Telatar, "Capacity of multi-antenna Gaussian channels," *Eur. Trans. Telecommun.*, vol. 10, no. 6, pp. 585-595, Nov. 1999.

[7] G. Carie and S. Shamai, "On the achievable throughput of a multiantenna Gaussian broadcast channel," *IEEE Trans. Inf. Theory,* vol. 49, no. 7, pp. 1691-1706, July 2003.

[8] P. Viswanath and D. Tse, "Sum capacity of the vector Gaussian broadcast channel and uplink-downlink duality," *IEEE Trans. Inf. Theory,* vol. 49, no. 8, pp. 1912-1921, Aug. 2003.

[9] S. Vishwanath, N. Jindal, and A. Goldsmith, "Duality, achievable rates, and sum-rate capacity of Gaussian MIMO broadcast channels," *IEEE Trans. Inf. Theory*, vol. 49, no. 10, pp. 2658-2668, Oct. 2003.

[10] W. Yu and J. M. Cioffi, "Sum capacity of Gaussian vector broadcast channels," *IEEE Trans. Inf. Theory,* vol. 50, no. 9, pp. 1875-1892, Sep. 2004.

[11] N. D. Sidiropoulos, T. N. Davidson, and Z.-Q. Luo, "Transmit beamforming for physical-layer multicasting," *IEEE Trans. Sig. Process.*, vol. 54, pp. 2239-2251, June 2006.

[12] N. Jindal and Z.-Q. Luo, "Capacity limits of multiple antenna multicast," in *Proc. IEEE Int. Symposium Inf. Theory (ISIT)*, pp. 1841-1845, 2006.

[13] T. Cover and J. Thomas, *Elements of information theory,* New York: Wiley, 1991.

[14] L. R. Varshney, "Unreliable and resource-constrained decoding," Ph.D. Thesis, EECS Department, MIT, June 2010.

[15] M. Gastpar, "On capacity under receive and spatial spectrum-sharing constraints," *IEEE Trans. Inf. Theory*, vol. 53, no. 2, pp. 471-487, Feb. 2007.

[16] R. Zhang and Y. C. Liang, "Exploiting multi-antennas for opportunistic spectrum sharing in cognitive radio networks," *IEEE J. S. Topics Sig. Process.*, vol. 2, no. 1, pp. 88-102, Feb. 2008.

[17] R. Zhang, Y. C. Liang, and S. Cui, "Dynamic resource allocation in cognitive radio networks," *IEEE Sig. Process. Mag.*, vol. 27, no. 3, pp. 102-114, May 2010.

[18] S. Boyd and L. Vandenberghe, *Convex optimization,* Cambridge University Press, 2004.

[19] J. Proakis, *Digital communication*, McGraw-Hill Science Press, 2000.

[20] S. Boyd, "Convex optimization II," Stanford University. Available [online] at http://www.stanford.edu/class/ee364b/lectures.html

[21] T. Le, K. Mayaram, and T. Fiez, "Efficient far-field radio frequency energy harvesting for passively powered sensor networks," *IEEE J. Solid-State Circuits*, vol. 43, no. 5, pp. 1287-1302, May 2008.

[22] V. R. Cadambe and S. A. Jafar, "Interference alignment and the degrees of freedom for the K user interference channel," *IEEE Trans. Inf. Theory*, vol. 54, no. 8, pp. 3425-3441, Aug. 2008.